

Evolutionary Origin of the Turtle Shell

Tyler R. Lyson,^{1,2,3,*} Gabe S. Bever,^{4,5} Torsten M. Scheyer,⁶ Allison Y. Hsiang,¹ and Jacques A. Gauthier^{1,3}

¹Department of Geology and Geophysics, Yale University, 210 Whitney Avenue, New Haven, CT 06511, USA

²Department of Vertebrate Zoology, National Museum of Natural History, Smithsonian Institution, Washington, DC 20560, USA

³Division of Vertebrate Paleontology, Yale Peabody Museum of Natural History, New Haven, CT 06511, USA

⁴New York Institute of Technology, College of Osteopathic Medicine, Old Westbury, NY 11568, USA

⁵Division of Paleontology, American Museum of Natural History, New York, NY 10024, USA

⁶Paläontologisches Institut und Museum, Universität Zürich, Karl-Schmid-Strasse 4, 8006 Zürich, Switzerland

Summary

The origin of the turtle shell has perplexed biologists for more than two centuries [1]. It was not until *Odontochelys semitestacea* [2] was discovered, however, that the fossil and developmental data [3–8] could be synthesized into a model [9] of shell assembly that makes predictions for the as-yet unestablished history of the turtle stem group. We build on this model by integrating novel data for *Eunotosaurus africanus*—a Late Guadalupian (~260 mya) [10] Permian reptile inferred to be an early stem turtle [11]. *Eunotosaurus* expresses a number of relevant characters, including a reduced number of elongate trunk vertebrae (nine), nine pairs of T-shaped ribs, inferred loss of intercostal muscles, reorganization of respiratory muscles to the ventral side of the ribs, (sub)dermal outgrowth of bone from the developing perichondral collar of the ribs, and paired gastralia that lack both lateral and median elements. These features conform to the predicted sequence of character acquisition and provide further support that *E. africanus*, *O. semitestacea*, and *Proganochelys quenstedti* represent successive divergences from the turtle stem lineage. The initial transformations of the model thus occurred by the Middle Permian, which is congruent with molecular-based divergence estimates [12–15] for the lineage, and remain viable whether turtles originated inside or outside crown Diapsida.

Results

Unlike the bony covering of other “shelled” amniotes (e.g., anguid lizards, ankylosaur dinosaurs, armadillos, and placodonts), the carapace of turtles is not simply a composite of dermal ossifications but rather integrates outgrowths of intramembranous bone from the perichondrium of the developing ribs and thoracolumbar vertebrae [3–8]. Whether the origin of the turtle shell also involved melding of overlying osteoderms (composite model) or not (de novo model) was vigorously

debated throughout the 20th and early 21st centuries (see [16]) with support falling largely along disciplinary lines [3–9, 17–25]. Paleontological explanations relied heavily on the composite model [19–25], but their efficacy was hampered by the large morphological gap separating the earliest, fully shelled turtles (e.g., *Proganochelys quenstedti* [26]) from all other known groups. In contrast, developmental biologists promoted the de novo model and viewed the lack of clear transitional fossils as support for a rapid evolution of the shell, perhaps coincident with the appearance of a bone morphogenetic protein (BMP) developmental pathway critical to shell construction in modern turtles [3–9, 27]. The lack of osteoderms in the recently discovered stem turtle *Odontochelys semitestacea* [2] strongly supports the de novo model of shell origination and liberates the paleontological search for the even deeper history of the turtle stem from its previously self-imposed constraint of osteoderm-bearing forms. For example, the long-recognized similarities between turtles and the osteoderm-free, Late Guadalupian Permian reptile *Eunotosaurus africanus* (Figure 1 and Figure S1 available online) [11, 23, 24, 28, 29] can now be viewed as homologous, with *Eunotosaurus* lying just deep to *Odontochelys* on the turtle stem [11]. Our study tests the role of *Eunotosaurus* in understanding the origin of turtles and their shell by determining whether its morphology conforms to the predictions of the Kuratani et al. [9] model of turtle shell evolution and development. To this end, we employ new specimens and novel data sources (including rib histology; Figures 1, 2, and 3 and the Supplemental Experimental Procedures) in a phylogenetic analysis of shell-related features (Figure 4 and the Supplemental Experimental Procedures). We summarize our results by expanding the Kuratani et al. [9] model to include the turtle stem deep to *Odontochelys*.

Morphology

GM 86/341 is the only specimen of *Eunotosaurus africanus* with a complete cervical and trunk vertebral series (see section I of the Supplemental Experimental Procedures for a complete list of the material examined). Nine elongated trunk vertebrae and nine pairs of dorsal ribs are clearly present, which differs from the traditional reconstruction of ten trunk vertebrae and ten pairs of ribs [23, 30, 31]. A distinct change in vertebral length, neural spine shape, and rib morphology occurs between presacral vertebrae 6 and 7 (Figures 1A–1C and S1A–S1C). We argue this is the transition between the cervical and trunk regions (sensu [32]). The cervical vertebrae are short with a bulbous neural spine [24]. They have long, slender ribs that are round in cross-section and unexpanded distally. Cervical rib 6 (dorsal rib 1 of other authors) is long and mostly round in cross-section except for a small, middle portion that is distinctly broadened. Thus, there are six, not five, cervical vertebrae and nine, not ten, dorsal vertebrae with nine pairs of distinctly broadened dorsal ribs. The dorsal ribs are T-shaped in cross-section and contact each other for most of their length. The first eight pairs are oriented slightly posteriorly, whereas the last pair projects slightly anteriorly. Unlike other specimens (USNM 23099, SAM 4328, and BMNH 4949), the last pair of ribs in GM 86/341 articulates with, but is not

*Correspondence: tyler.lyson@gmail.com

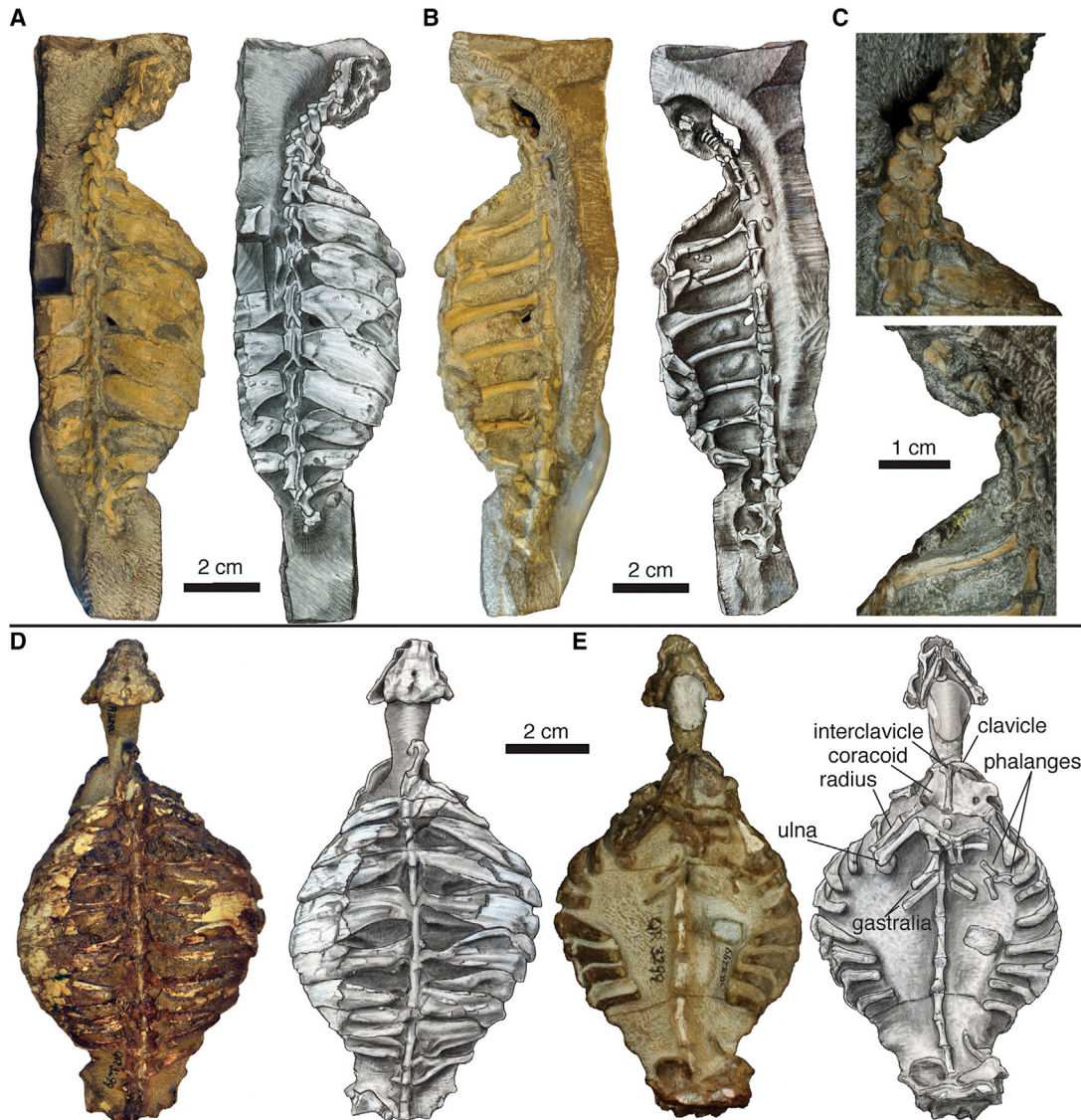


Figure 1. Newly Described *Eunotosaurus africanus* Material

(A) Photograph (left) and illustration (right) of GM 86/341 in dorsal view.

(B) Photograph (left) and illustration (right) of GM 86/341 in ventral view.

(C) Close-up photographs of the neck region of GM 86/341 in dorsal (top) and ventral (bottom) views showing differences between cervical (short centra with bulbous neural spines, and elongate ribs) and dorsal (greatly elongate centra, with long neural spines, and anteroposterior broadened ribs) vertebrae.

(D) Photograph (left) and illustration (right) of QR 3299 in dorsal view.

(E) Photograph (left) and illustration (right) of QR 3299 in ventral view.

See also [Figure S1](#) for red/blue stereophotographs of each specimen.

fused to, the corresponding vertebra. That this condition reflects size/age variation is supported by the smaller size of GM 86/341.

Several specimens preserve a complete, articulated shoulder girdle (AM 5999, NMQR 3299, GM 777, SAM K 1133, and SAM K 7909). The scapula is situated vertically and rostral to the dorsal ribcage ([Figures S1D and S1E](#)). The clavicles are slender elements with a distinct dorsal process ([Figure S1E](#)). A slender cleithrum, which was hypothesized by Cox [23], is confirmed. Its ventral end contacts the dorsal tip of the clavicle ([Figure S1E](#)). Paired gastralia lacking lateral and medial element(s) are preserved in NMQR 3299 ([Figures 1F and S1C](#)) and BP/1/7024.

Microanatomy and Histology

The dorsal ribs of *Eunotosaurus africanus* ([Figures 2B, 2F, and S2](#)) and *Proganochelys quenstedti* ([Figure 2G](#)) are T-shaped in cross-section (longitudinal or parasagittal section in reference to the body axis) proximally, with a broadened surface and a rounded visceral aspect that is arranged vertically ([Figure 2B](#)). In both taxa, the vertical portion of the “T” includes a gentle bulge distally ([Figures 2F and 2G](#); see [33]).

In GM 86/341, the anterior-most part of the broadened part of the rib deviates ventrally and tapers to a sharp edge so that the outer bone surface is straight to slightly concave. The posterior part does not deviate ventrally but maintains a constant thickness, and it ends in an upturned blunt tip such

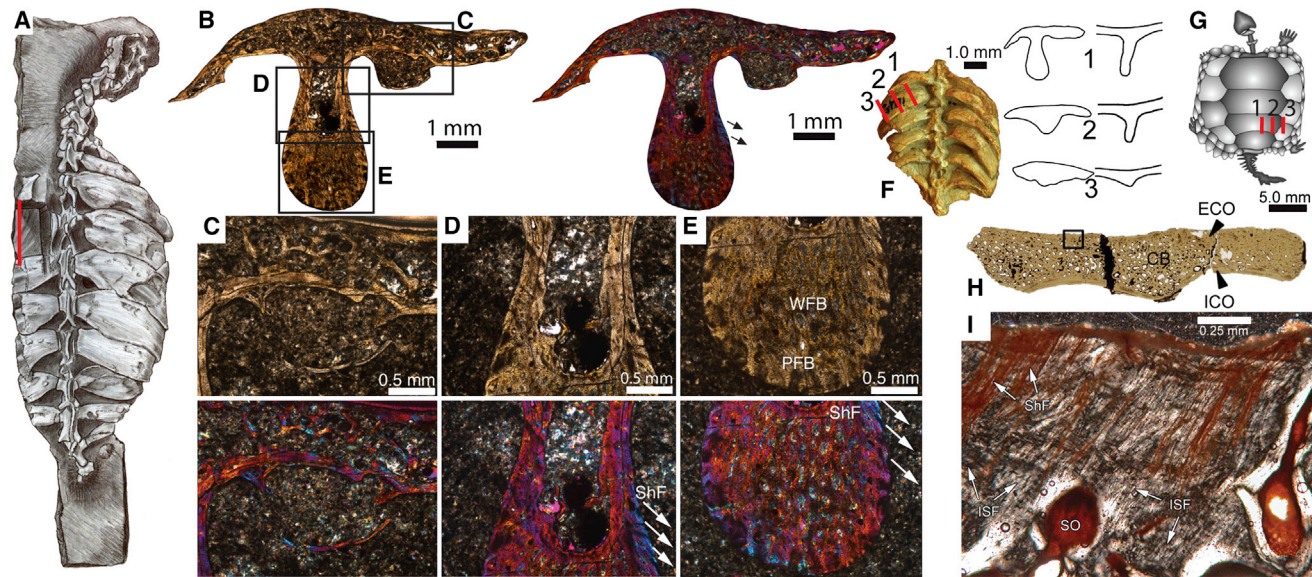


Figure 2. Histological Data from the Ribs of *Eunosaurus africanus* and *Proganochelys quenstedti*

(A) Illustration of *Eunosaurus* (GM 86/341) showing where the left third dorsal rib was sectioned histologically (red line).

(B) Histological section in normal (left) and polarized (right) light showing the T shape of the rib in cross-section (see “1” in F, which shows the approximate place the histological section was taken as compared to where the section was taken for *Proganochelys*). Black arrows indicate the presence and orientation of Sharpey’s fibers.

(C–I) Images in (C), (D) and (E) are seen in normal transmitted (upper) and cross-polarized light using a lambda compensator (lower). Image in (H) is seen in normal transmitted and the one in (I) is seen in cross-polarized light.

(C) Close-up view of the posterior diploe portion of the T-shaped rib. Thin external and internal compact layers frame interior cancellous bone, which is composed of thin trabeculae. Note the thin ring-like structure at internal (visceral) surface of the rib.

(D) Close-up view of the midshaft region of the rib. Note central ovoid cavity surrounded by periosteal parallel-fibered bone (PFB). Sharpey’s fibers (ShF) are present in the posterior part of this region (blue colors). White arrows indicate the orientation of insertion of the ShF.

(E) Close-up of the drop-shaped bulge, which consists internally of highly vascularized woven bone tissue (WFB) and externally of PFB. Sharpey’s fibers (white arrows) are absent from the anterior and ventral parts of the bulge. White arrows indicate presence and orientation of Sharpey’s fibers.

(F and G) *Eunosaurus* specimen (F, left; GM 71) showing the change in cross section of the rib (F, right) as you move distally compared to the change in cross section of the rib/costal morphology (G, left) of *Proganochelys* (G, right).

(H) Histological section of *Proganochelys* (MB.R. 3449.2) taken from the right costal 7? at approximately level three (see the corresponding number in G).

(I) Close-up view of the external cortex, which is composed mainly of interwoven structural fibers (ISF). Numerous parallel Sharpey’s fibers insert into the bone tissue at high angles (ShF). A few scattered secondary osteons (SO) are visible.

See also [Figure S2](#).

that the internal (visceral) bone surface is slightly convex. A tapering anterior portion cannot be confirmed in NHM PV R 4949, but its posterior portion is either horizontal or slightly downturned due to its more posterior position in the trunk. Three phases of bone deposition, an initial phase and two successive phases, are recognizable (see section II of the [Supplemental Experimental Procedures](#)). No interwoven dermal structural fibers or remnants of cartilage are apparent anywhere in the sectioned rib.

Although of similar overall size, both sectioned *Eunosaurus* ribs differ somewhat in cortical bone thickness, as well as in internal trabecular thickness and arrangement, with NHM PV R 4949 appearing more robust overall. In this specimen, growth marks are visible in the cortical bone as light and dark banding in normal transmitted light, but histological details (e.g., Sharpey’s fibers) are otherwise not well preserved. The source of these variations is unclear.

Three discrete phases of bone deposition are visible, an initial and two successive phases (see the [Supplemental Experimental Procedures](#) for a detailed histological description). In the initial phase, a central large cavity (representing the rib primordium) gets encased by parallel-fibered bone (PFB). In the next phase, thin sheets of anteriorly and posteriorly extending bone are added dorsally and interior trabeculae

spread out from the bone around the central ovoid cavity, thus creating a diploe structure. In the final phase, the drop-shaped bulge of the ventral shaft of the T-shaped rib is deposited laterally and ventrally to the initial tube structure. During growth, inconspicuous Sharpey’s fibers are locally present only at the posterior margin of the ventral shaft.

Phylogenetic Analysis

Fifteen morphological characters and one taxon, the shelled *Sinosauropsphargis yunguiensis*, were added to the morphological data set of Lyson et al. [11] ([Supplemental Experimental Procedures](#), sections III–VI). In turn, this data set is that of deBraga and Rieppel [34], with Li et al.’s [2] addition of *Odontochelys semitestacea* and one morphological character and Lyson et al.’s [11] addition of *Eunosaurus africanus* and *Proganochelys quenstedti* and seven morphological characters. Two most parsimonious trees (confidence interval [CI] = 0.3333, retention index = 0.6785, consistency index = 0.2262) with 723 steps were obtained ([Figure S3](#)). In addition, we performed a Bayesian phylogenetic analysis, and the resulting topology is identical to that of the parsimony analysis. There is strong support for a turtle + *Eunosaurus* clade (bootstrap = 69% and posterior probability = 95%).

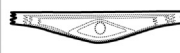
A		circular cartilaginous rib primordia (based on extant tetrapod embryos)		ovoid (?) cartilaginous rib primordia		circular cartilaginous rib primordia
B		development of periosteum; no periosteal outgrowths into adjacent subdermal tissue		development of periosteum; initial outgrowth of bone spiculae from rib periosteum into adjacent subdermal tissue		development of periosteum; initial outgrowth of bone spiculae from rib periosteum into adjacent dermal tissue
C		continued deposition of periosteal bone layers (rib shape can differ depending on taxon); development of medullary cavity		formation of dorsal (horizontal) blade of T-shaped diploe part of rib through periosteal and appositional bone growth		early formation of costal around the initial rib through incorporation of preformed dermal tissue structures indicates switch from periosteal to metaplastic ossification (early costal shape can differ depending of taxon)
D	 generalized terrestrial tetrapod rib	continued deposition of periosteal bone layers until skeletal maturity is reached (rib shape can differ depending on taxon); increase in diameter of medullary cavity usually in equilibrium with new periosteal bone formation	 <i>Eunotosaurus</i> rib	subsequent formation of visceral (vertical) drop-shaped bulge of rib; adjacent ribs overlap and abut each other but lack sutures; earlier growth stages of the dorsal blade part of rib are completely remodelled	 generalized turtle costal	growth of costal plate through metaplastic ossification; continued growth throughout ontogeny enabled through sutures; depending on the species, traces of rib and subsequent costal plate growth stages can get lost through remodelling processes (costal shape can differ depending of taxon)

Figure 3. Comparative Rib Development in Amniotes

The first stage of development is similar in the three groups (left, generalized amniote; middle, *Eunotosaurus africanus*; and right, generalized turtle). (Sub)dermal outgrowth of bone from the perichondral/periosteal collar of the developing rib is a developmental feature shared by *Eunotosaurus* and turtles. *Eunotosaurus* exhibits subsequent stages of rib development that we interpret as autoapomorphic. See also Figure S2.

Discussion

Eunotosaurus, which previously was excluded from global analyses of amniote relationships, was recently recovered as sister to undisputed turtles [11]. Likewise, the addition of turtles to the latest “parareptile” data set (i.e., [35]) yields a *Eunotosaurus* + turtle clade [11]. The previously undescribed *Eunotosaurus* material provides compelling additional morphological support for a privileged relationship with turtles.

Strengthening Support for a Turtle-*Eunotosaurus* Clade

Our examination of previously undescribed specimens of *Eunotosaurus*, as well as the comparative histology of *Eunotosaurus* ribs, strengthens support for *Eunotosaurus* as both a stem turtle and a critical transitional form in the evolution of the turtle body plan. Gross morphological features related to the shell that are shared between *Eunotosaurus* and turtles now include trunk vertebrae reduced to nine (shared with *Odontochelys*), nine pairs of broadened dorsal ribs (shared with *Odontochelys semitestacea* and *Proganochelys quenstedti*), elongation of trunk vertebrae with length exceeding width by four times or more (shared with all undisputed stem and crown turtles), cross-section of ribs T-shaped proximally developing into a gentle ventral bulge distally (shared with several early turtles, including *O. semitestacea* [2], *P. quenstedti* [26], and *Palaeochersis talampayensis* [36]), and paired gastralia that do not overlap medially and lack both a central medial element and lateral element(s) (shared with all turtles and parareptiles in which gastralia are preserved, and lacking in all diapsids that have a central medial and/or lateral element(s); e.g., [37]). Each of these characters optimizes as unambiguous synapomorphies of *Eunotosaurus* and undisputed turtles among reptiles. In addition, the cartilaginous rib primordium of *Eunotosaurus* changes position in relation to the developing T-shaped rib, which is also the case in the developing costals of hard-shelled turtles [38] (Figure S2). In both *Eunotosaurus* and hard-shelled turtles, the proximal end of the primordial rib cartilage is situated more dorsally, whereas distally it becomes progressively ventral, finally touching the internal cortical bone (NHM PV R 4949; Figure S2). It should be noted that this change in position of the primordial rib cartilage is not seen in the trionychid *Apalone ferox* (Figure S2), in which the primordial rib cartilage maintains a fairly constant position. This appears to be an autapomorphy for soft-shelled turtles.

The morphology of *Eunotosaurus* is consistent with the explicit prediction of Kuratani et al. [9] that the early stages of the turtle shell, prior to the emergence of *Odontochelys*,

was marked by a vertical scapula positioned rostral to the ribcage. This condition is expressed in *Eunotosaurus*, in contrast to some other putative turtle sister groups, which have a scapula dorsal to the ribcage (see [39]). Furthermore, the gross morphology of *Eunotosaurus* only differs from undisputed stem turtles, such as *Odontochelys*, in sharing fewer derived characters with crown turtles, as would be expected for an earlier member of the turtle stem. For example, *Eunotosaurus* lacks the derived conditions of neural plates, a hypoischium, and a co-ossified plastron (though all of the bones that form the plastron are present in *Eunotosaurus*).

The rib histology of *Eunotosaurus* provides further support for a sister-group relationship with undisputed turtles (Figures 2, 3, and S2). The nature of the bone tissue found in the horizontal flange and the shaft region of the rib is compatible with periosteal and appositional bone growth (“Zuwachsknochen” sensu [40]). The histological data indicate three phases of bone morphogenesis in *Eunotosaurus* (Figure 3). Periosteal bone is first deposited around a circular to ovoid cartilaginous rib primordium and is then followed by successive resorption of the cartilage tissue. This phase is found in all amniotes examined thus far. Second, outgrowth of bone trabeculae and bony sheets forms the dorsally broadened, horizontal flange part of the rib. Such outgrowth of dermal bone from the developing perichondral/periosteal collar of the rib is a unique synapomorphy (CI = 1.00) of *Eunotosaurus* and turtles. Finally, the visceral portion of the rib is reinforced by successive deposition of parallel fibered periosteal and woven endosteal bone, and remodeling processes of the dorsal diploe structure set in. This last phase of bone development differs profoundly from all other amniotes examined and is considered an autapomorphy of *Eunotosaurus*. There is no evidence of metaplastic ossification at any stage of rib formation, unlike in undisputed turtles in which the costals incorporate interwoven structural fibers (i.e., metaplastically ossified integumentary layer [33, 41]). However, this stage of costal development normally occurs late in development, mostly posthatchling [5]. Thus, the absence of this feature might be expected deep in the turtle stem, especially if the feature evolved through terminal addition at some point between the divergence of *Eunotosaurus* and *Proganochelys*.

The local presence of Sharpey’s fibers at only the posterior part of the ventral shaft in both the first and second successive phase of bone deposition is here interpreted as an insertion of respiratory or locomotory muscles (or associated ligaments) into the rib, which stayed active throughout the ontogenetic timeframe recorded in the thin sections. The Sharpey’s fibers are not considered indicative of intercostal muscles because they are only found on the posterior portion of the rib, and

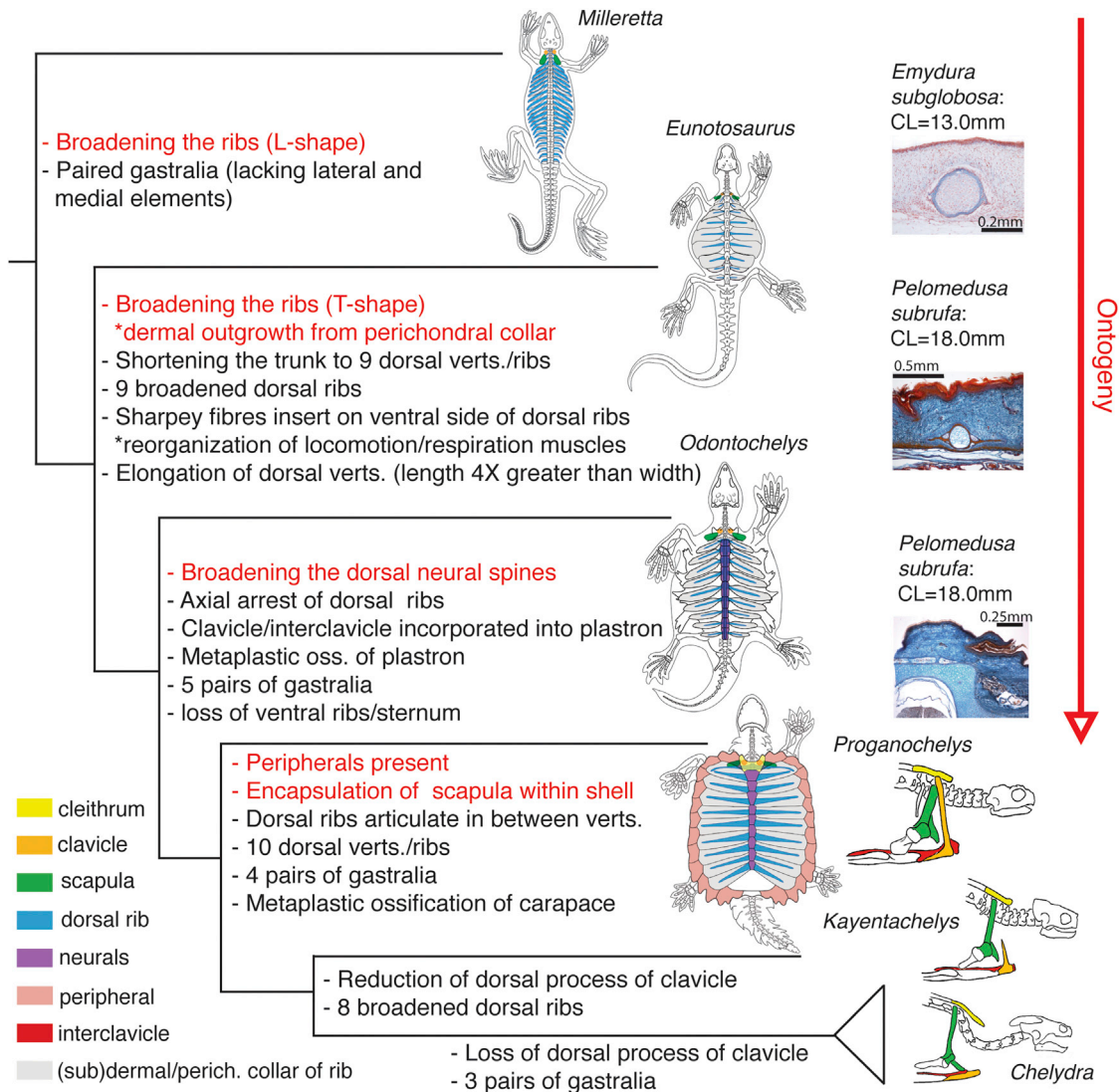


Figure 4. Evolutionary Developmental Model for the Origin of the Turtle Shell

Results of a phylogenetic analysis of shelled reptiles and characters important in constructing a shell are plotted against the ontogeny of pleurodire turtles. Thin sections through turtle embryos show the initial outgrowth of (sub)dermal bone through the costals first (carapace length [CL] = 13.0 mm in the pleurodire *Emydura subglobosa*) and then the neurals (CL = 18.0 mm in the pleurodire *Pelomedusa subrufa*). The timing of ontogenetic transformations of those features (in red) important in the construction of the shell (i.e., the number of dorsal vertebrae or ribs does not change through ontogeny) is congruent with the phylogenetic transformation of those same features based on our recovered tree topology. Our model makes explicit morphological and histological predictions for the lineage prior to the most recent common ancestor of *Eunotosaurus africanus* and turtles that are met by the morphology found in *Milleretta rubidgei*. Numbers above each node represent bootstrap frequencies obtained in the phylogenetic analysis. See section VIII of the [Supplemental Experimental Procedures](#) for justification for each reconstruction. See also [Figures S3 and S4](#).

intercostal muscles normally insert on both the anterior and posterior portion of the ribs (Figure S2). Furthermore, even in animals with anteroposterior broadened ribs and poorly developed intercostal musculature (e.g., the mammal *Cyclopes didactylus*; Figure S2), Sharpey's fibers are still present on both the anterior and posterior surfaces of the rib. Thus, the restriction of Sharpey's fibers to the posterior side of the rib is an unambiguous synapomorphy (CI = 1.00) shared only with turtles. We interpret these fibers to reflect not an intercostal muscle per se, but rather a muscle used in locomotion or more directly in respiration. Given the observation that the dermis in turtles completely ossifies, numerous muscles involved in locomotion (e.g., *m. testocoracoideus*) and respiration (e.g., *m. diaphragmaticus* and *m. transversus*

abdominis) are obliged to insert on the ventral portion of the ribs. This differs from other amniote ribs, in which intercostal muscles extend between the ribs, with no muscles inserting on the ventral face of the rib [42, 43] (Figure S2).

Expansion of the Kuratani Model

Given the inference of *Eunotosaurus* as the sister to turtles in phylogenetic analyses of both amniotes and "parareptiles" [11], the numerous unique morphologic and developmental synapomorphies it shares with turtles, and its congruence with the transformational model outlined by Kuratani et al. [9], we here incorporate *Eunotosaurus* into an expanded evolutionary developmental model for the origination of the turtle shell. Kuratani et al. [9] used the timing of development

of key shell features to predict ancestral morphologies and secondarily place fossils within this developmental framework (Supplemental Experimental Procedures, section VII). We extend this model to include the developmental timing of a more comprehensive list of individual characters that are essential to building a turtle shell (Figure 4). Outgrowth of membrane bone from the perichondral/periosteal collar of the developing rib occurs first, followed by outgrowth of bone from the neural spines of the trunk vertebrae, and finally by the acquisition of peripheral bones and the encapsulation of the scapula within the shell [7, 8] (Figure 4). The phylogenetic sequence exhibited by *Eunotosaurus* (broadened ribs T-shaped in cross-section, dermal outgrowth of bone from the perichondral/periosteal collar of the rib, and reorganization of locomotion and respiratory muscles), *Odontochelys* (broadened neurals), and *Proganochelys* (acquisition of peripherals and encapsulation of scapula within shell) is consistent with the evolutionary developmental model. This expanded model pulls the initial transformations of the turtle shell back to at least the late Middle Permian. But, this is still younger than all recent molecular-based divergence estimates for Pan-Testudines [12, 13] and thus is viable irrespective of whether turtles originated inside or outside of crown Diapsida. To be clear, our phylogenetic analysis does recover the *Eunotosaurus* + turtle clade outside Diapsida, which places it in conflict with molecular based topologies [12–15].

Our model for the origin of the turtle shell makes a number of morphological and histological predictions for stem turtles that existed or diverged prior to the most recent common ancestor of *Eunotosaurus* and extant turtles. For example, based on the early development of outgrowth of membrane bone from the ribs of extant turtles (e.g., [38]), the model predicts that earlier stem turtles had slightly broadened ribs with some intramembranous outgrowth of bone from the perichondral/periosteal collar of the rib. Based on the inference that the unique abdominal muscle ventilation system of turtles [44], in which the muscles attach to the ventral portion of the carapace [45], arose from a basal amniote with costal ventilation [46], the model also predicts that early stem turtles likely had both intercostal muscles (unlike *Eunotosaurus*) and muscles beginning to insert on the ventral side of the trunk/dorsal ribs. Histological data for *Milleretta rubidgei* has yet to be obtained, but this moderately broad-ribbed species, inferred in phylogenetic analyses to have diverged from the turtle stem earlier than *Eunotosaurus* [11, 30, 47], meets many of these morphological predictions (Figure 4). The dorsal ribs of *Milleretta* display an intermediate condition between the rod-like ribs found in stem amniotes (i.e., *Limnoscelis paludis*) and the broad ribs found in *Eunotosaurus* and *Odontochelys*. We look forward to testing the predictions of the expanded model through further study of this taxon.

Supplemental Information

Supplemental Information includes Supplemental Experimental Procedures and four figures and can be found with this article online at <http://dx.doi.org/10.1016/j.cub.2013.05.003>.

Acknowledgments

We thank the following institutions and their curators/staff for access to material under their care: Albany Museum (Grahamstown), Natural History Museum (London), Institute of Paleontology and Paleoanthropology (Beijing), Council for Geosciences (Pretoria), National Museum

(Bloemfontein), Bernard Price Institute (Johannesburg), South African Museum (Cape Town), Staatliches Museum für Naturkunde (Stuttgart), United States National Museum (Washington, D.C.), and Yale Peabody Museum of Natural History (New Haven). M. Fox (Yale Peabody Museum [YPM]) is thanked for her careful preparation of the fossil material. B. Roach (YPM) made the beautiful illustrations used herein. W. Joyce is thanked for his help with Figure 2. The vertebrate paleontology group at the PIMUZ is thanked for various assistances and discussions. K. deQueiroz, M.S.Y. Lee, M. Laurin, and an anonymous reviewer had useful comments that improved the manuscript. External funding for this project was provided by an NSF Graduate Research Fellowship and a Smithsonian Institution Peter Buck Fellowship to T.R.L. and a Swiss National Science Foundation grant (SNSF no. 31003A_127053) to T.M.S.

Received: January 3, 2013

Revised: April 3, 2013

Accepted: May 1, 2013

Published: May 30, 2013

References

- Agassiz, L. (1857). Contributions to the Natural History of the United States of America (Boston: Little, Brown and Company).
- Li, C., Wu, X.-C., Rieppel, O., Wang, L.-T., and Zhao, L.-J. (2008). An ancestral turtle from the Late Triassic of southwestern China. *Nature* 456, 497–501.
- Burke, A.C. (1989). Development of the turtle carapace: implications for the evolution of a novel bauplan. *J. Morphol.* 199, 363–378.
- Burke, A.C. (1991). The development and evolution of the turtle body plan. Inferring intrinsic aspects of the evolutionary process from experimental embryology. *Am. Zool.* 31, 616–627.
- Gilbert, S.F., Loredó, G.A., Brukman, A., and Burke, A.C. (2001). Morphogenesis of the turtle shell: the development of a novel structure in tetrapod evolution. *Evol. Dev.* 3, 47–58.
- Cebra-Thomas, J., Tan, F., Sístla, S., Estes, E., Bender, G., Kim, C., Riccio, P., and Gilbert, S.F. (2005). How the turtle forms its shell: a paracrine hypothesis of carapace formation. *J. Exp. Zool. B Mol. Dev. Evol.* 304, 558–569.
- Gilbert, S.F., Cebra-Thomas, J.A., and Burke, A.C. (2008). How the turtle gets its shell. In *Biology of Turtles*, J. Wyneken, M.H. Godfrey, and V. Bels, eds. (Boca Raton: CRC Press), pp. 1–16.
- Sánchez-Villagra, M.R., Müller, H., Sheil, C.A., Scheyer, T.M., Nagashima, H., and Kuratani, S. (2009). Skeletal development in the Chinese soft-shelled turtle *Pelodiscus sinensis* (Testudines: Trionychidae). *J. Morphol.* 270, 1381–1399.
- Kuratani, S., Kuraku, S., and Nagashima, H. (2011). Evolutionary developmental perspective for the origin of turtles: the folding theory for the shell based on the developmental nature of the carapacial ridge. *Evol. Dev.* 13, 1–14.
- Rubidge, B.S., Erwin, D.H., Ramezani, J., Bowering, S.A., and de Klerk, W.J. (2013). High-precision temporal calibration of Late Permian vertebrate biostratigraphy: U-Pb zircon constraints from the Karoo Supergroup, South Africa. *Geology* 41, 363–366.
- Lyson, T.R., Bever, G.S., Bhullar, B.A.S., Joyce, W.G., and Gauthier, J.A. (2010). Transitional fossils and the origin of turtles. *Biol. Lett.* 6, 830–833.
- Hugall, A.F., Foster, R., and Lee, M.S.Y. (2007). Calibration choice, rate smoothing, and the pattern of tetrapod diversification according to the long nuclear gene RAG-1. *Syst. Biol.* 56, 543–563.
- Shen, X.-X., Liang, D., Wen, J.Z., and Zhang, P. (2011). Multiple genome alignments facilitate development of NPCL markers: a case study of tetrapod phylogeny focusing on the position of turtles. *Mol. Biol. Evol.* 28, 3237–3252.
- Crawford, N.G., Faircloth, B.C., McCormack, J.E., Brumfield, R.T., Winker, K., and Glenn, T.C. (2012). More than 1000 ultraconserved elements provide evidence that turtles are the sister group of archosaurs. *Biol. Lett.* 8, 783–786.
- Lyson, T.R., Sperling, E.A., Heimberg, A.M., Gauthier, J.A., King, B.L., and Peterson, K.J. (2012). MicroRNAs support a turtle + lizard clade. *Biol. Lett.* 8, 104–107.
- Lyson, T.R., and Gilbert, S.F. (2009). Turtles all the way down: loggerheads at the root of the chelonian tree. *Evol. Dev.* 11, 133–135.
- Nagashima, H., Kuraku, S., Uchida, K., Ohya, Y.K., Narita, Y., and Kuratani, S. (2007). On the carapacial ridge in turtle embryos: its

- developmental origin, function and the chelonian body plan. *Development* **134**, 2219–2226.
18. Nagashima, H., Sugahara, F., Takechi, M., Ericsson, R., Kawashima-Ohya, Y., Narita, Y., and Kuratani, S. (2009). Evolution of the turtle body plan by the folding and creation of new muscle connections. *Science* **325**, 193–196.
 19. Hay, O.P. (1922). On the phylogeny of the shell of the Testudinata and the relationships of *Dermochelys*. *J. Morphol.* **36**, 421–445.
 20. Gregory, W.K. (1946). Pareiasaurs versus placodonts as near ancestors to the turtles. *Bulletin of the American Museum of Natural History* **86**, 275–326.
 21. Lee, M.S.Y. (1997). Reptile relationships turn turtle. *Nature* **389**, 245–246.
 22. Joyce, W.G., Lucas, S.G., Scheyer, T.M., Heckert, A.B., and Hunt, A.P. (2009). A thin-shelled reptile from the Late Triassic of North America and the origin of the turtle shell. *Proc. Biol. Sci.* **276**, 507–513.
 23. Cox, C.B. (1969). The problematic Permian reptile *Eunotosaurus*. *Bull. Brit. Mus. Nat. Hist.* **18**, 165–196.
 24. Gow, C.E., and de Klerk, B. (1997). First record of *Eunotosaurus* (Amniota: Parareptilia) from the Eastern Cape. *Palaeontologia Africana* **34**, 27–31.
 25. Hill, R.V. (2005). Integration of morphological data sets for phylogenetic analysis of Amniota: the importance of integumentary characters and increased taxonomic sampling. *Syst. Biol.* **54**, 530–547.
 26. Gaffney, E.S. (1990). The comparative osteology of the Triassic Turtle *Proganochelys*. *Bulletin of the American Museum of Natural History* **194**, 1–263.
 27. Rieppel, O. (2001). Turtles as hopeful monsters. *Bioessays* **23**, 987–991.
 28. Seeley, H. (1892). On a new reptile from Welte Vreden (Beaufort West) *Eunotosaurus africanus* (Seeley). *Quarterly Journal of the Geological Society* **48**, 583–585.
 29. Watson, D.M.S. (1914). *Eunotosaurus africanus* Seeley, and the ancestry of the Chelonia. *Proceedings of the Zoological Society of London* **1914**, 1011–1020.
 30. Gow, C.E. (1997a). A reassessment of *Eunotosaurus africanus* Seeley (Amniota: Parareptilia). *Palaeontologia Africana* **34**, 33–42.
 31. Müller, J., Scheyer, T.M., Head, J.J., Barrett, P.M., Werneburg, I., Ericson, P.G.P., Pol, D., and Sánchez-Villagra, M.R. (2010). Homeotic effects, somitogenesis and the evolution of vertebral numbers in recent and fossil amniotes. *Proc. Natl. Acad. Sci. USA* **107**, 2118–2123.
 32. Gauthier, J.A., Kearney, M., Maisano, J.A., Rieppel, O., and Behlke, A. (2012). Assembling the squamate Tree of Life: perspectives from the phenotype and the fossil record. *Bulletin of the Peabody Museum of Natural History* **53**, 3–308.
 33. Scheyer, T.M., and Sander, P.M. (2007). Shell bone histology indicates terrestrial palaeoecology of basal turtles. *Proc. Biol. Sci.* **274**, 1885–1893.
 34. DeBraga, M., and Rieppel, O. (1997). Reptile phylogeny and the affinities of turtles. *Zool. J. Linn. Soc.* **120**, 281–354.
 35. Müller, J., and Tsuji, L.A. (2007). Impedance-matching hearing in Paleozoic reptiles: evidence of advanced sensory perception at an early stage of amniote evolution. *PLoS ONE* **2**, e889.
 36. Sterli, J., Rafael, S., de la Fuente, M.S., and Rougier, G.W. (2007). Anatomy and relationships of *Palaeochersis talampayensis*, a Late Triassic turtle from Argentina. *Palaeontographica Abteilung A* **281**, 1–61.
 37. Dilkes, D.W. (1998). The Early Triassic rhynchosaur *Mesosuchus browni* and the interrelationships of basal archosauromorph reptiles. *Philos. Trans. R. Soc. Lond. B Biol. Sci.* **353**, 501–541.
 38. Scheyer, T.M., Brüllmann, B., and Sánchez-Villagra, M.R. (2008). The ontogeny of the shell in side-necked turtles, with emphasis on the homologies of costal and neural bones. *J. Morphol.* **269**, 1008–1021.
 39. Lyson, T.R., and Joyce, W.G. (2012). Evolution of the turtle bauplan: the topological relationship of the scapula relative to the ribcage. *Biol. Lett.* **8**, 1028–1031.
 40. Starck, D. (1979). *Vergleichende Anatomie der Wirbeltiere, Volume 2* (Berlin: Springer).
 41. Scheyer, T.M., Sander, P.M., Joyce, W.G., Böhme, W., and Witzel, U. (2007). A plywood structure in the shell of fossil and living soft-shelled turtles (Trionychidae) and its evolutionary implications. *Organisms Diversity & Evolution* **7**, 136–144.
 42. Jenkins, F.A., Jr. (1970). Anatomy and function of expanded ribs in certain edentates and primates. *J. Mammal.* **51**, 288–301.
 43. Tsuihiji, T. (2007). Homologies of the longissimus, iliocostalis, and hypaxial muscles in the anterior presacral region of extant diapsida. *J. Morphol.* **268**, 986–1020.
 44. Landberg, T., Mailhot, J.D., and Brainerd, E.L. (2003). Lung ventilation during treadmill locomotion in a terrestrial turtle, *Terrapene carolina*. *J. Exp. Biol.* **206**, 3391–3404.
 45. Shah, R.V. (1962). A comparative study of the respiratory muscles in Chelonia. *Brevoria* **161**, 1–16.
 46. Brainerd, E.L., and Owerkowicz, T. (2006). Functional morphology and evolution of aspiration breathing in tetrapods. *Respir. Physiol. Neurobiol.* **154**, 73–88.
 47. Tsuji, L.A., and Müller, J. (2009). Assembling the history of the Parareptilia: phylogeny, diversification, and a new definition of the clade. *Fossil Record* **12**, 71–81.

Current Biology, Volume 23

Supplemental Information

Evolutionary Origin of the Turtle Shell

Tyler R. Lyson, Gabe S. Bever, Torsten M. Scheyer, Allison Y. Hsiang, and Jacques A. Gauthier

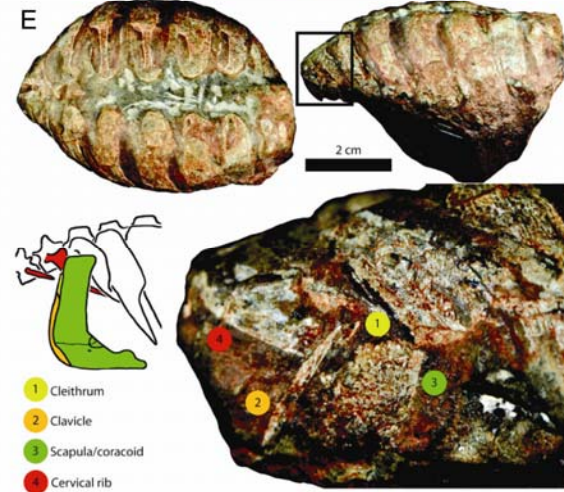
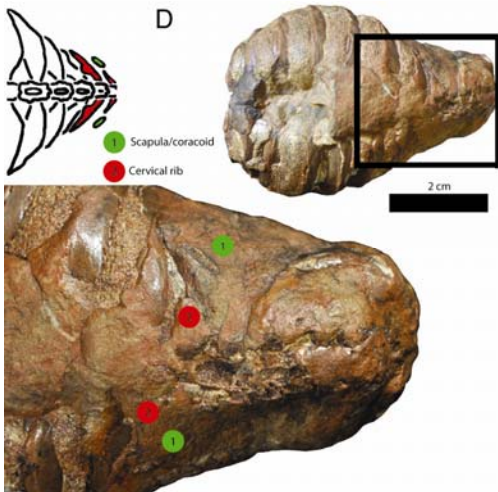
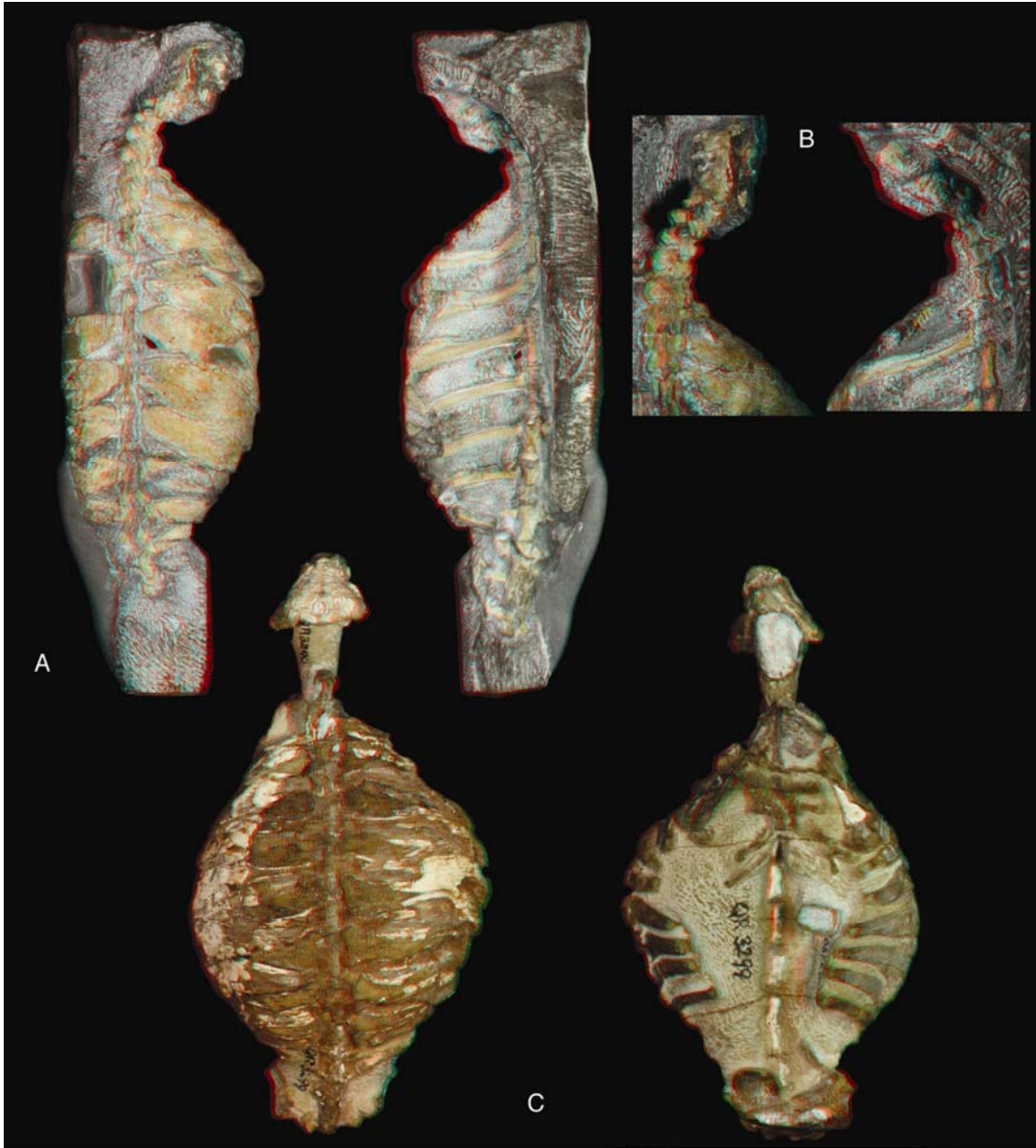


Figure S1. *New Eunotosaurus africanus material, Related to Figure 1*

A) Red/blue stereophotographs of GM 86/341 in dorsal (left) and ventral (right) views. B) Close-up red/blue stereophotographs (bottom) of the neck region of GM 86/341 in dorsal (top) and ventral (bottom) views showing the differences between cervical (short centra with bulbous neural spines, and elongate ribs) and dorsal (greatly elongate centra, with long neural spines, and anterior-posterior broadened ribs) vertebrae. C) Red/blue stereophotographs of QR 3299 in dorsal (left) and ventral (right) views. D) Photographs of *E. africanus* (SAM K 7909) in dorsal view (top right), with a close-up of the shoulder girdle region showing the vertical nature of the scapula rostral to the dorsal ribs. E) Photographs of *E. africanus* (SAM K 1133) in dorsal (top left) and lateral (top right) with a close-up (bottom right) of the shoulder girdle region showing the vertical nature of the scapula rostral to the dorsal ribs. A small, but distinct, cleithrum is also present.

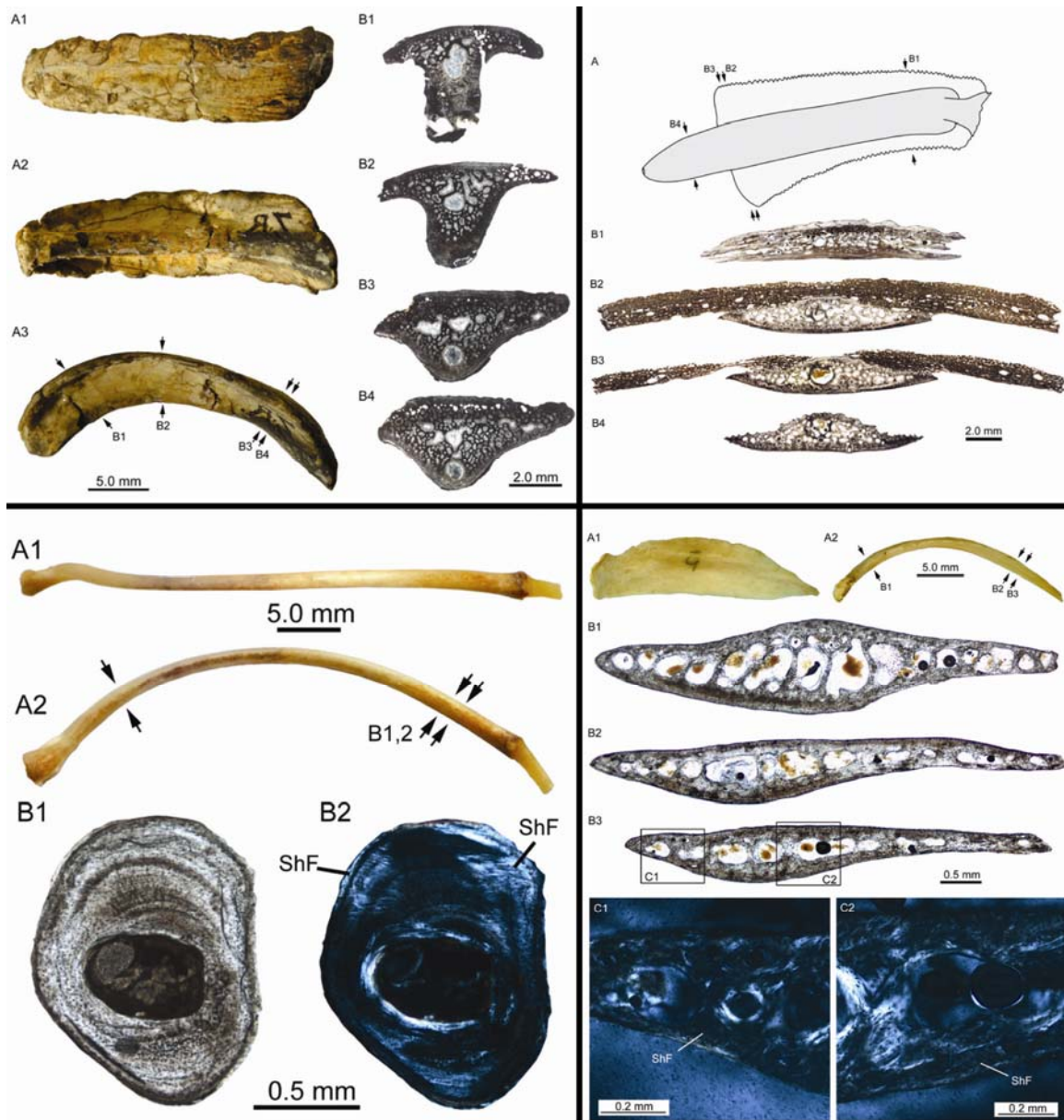


Figure S2. Histological data of various amniote ribs, Related to Figures 2 and 3
Top left) *Eunosaurus africanus* left dorsal rib 7 (NHM PV R 4949). A1-A3) Gross anatomy of the rib in A1) dorsal, A2) ventral and A3) lateral view. Black arrows mark the planes of histological sectioning (B1-B4). Proximal is to the right in A1 and A2 and to the left in A3. B1-B4) Proximodistal series of planes of sectioning in normal transmitted light. The position of the central circular cavity, indicating the progression of the primordial rib cartilage, changes from dorsal towards ventral within the T-shaped rib. The central cavity in B1 appears ovoid because of remodelling of surrounding bone tissue.
Top right) *Apalone spinifera* costal 6 (YPM HERR.010586). A) Schematic drawing of costal in ventral view (not to scale, proximal to the right), with black arrows marking the planes of sectioning shown in B1-B4. Note distal circular opening at the tip of the free rib end. Light grey, dermal costal plate; dark grey, incorporated endoskeletal rib. B1-B4)

Proximodistal sections in normal transmitted light. Note that the diameter of the cartilaginous rib primordium (marked by the larger, round central cavity) is smaller proximally and increases distally. B1) Proximal section of costal. A ventral rib bulge is indistinguishable from the costal plate. B2) First distal section. The ventral 'rib part' is clearly separable from the overlying flat, dermal part of the costal. The plywood pattern typically found in the external cortex of trionychid shell bones [41] is largely incorporated, but the overlying ornamentation pattern of ridges and valleys is not yet developed. B3) Second distal section through the distal-most extensional front of costal growth. The plywood-like pattern is just being incorporated into the external cortex of the costal. Note scalloped dorsal surface and smooth ventral surface of the rib. B4) Section through free-end part of the rib. The structures of this part are reminiscent of the ventral 'rib part' seen in B3 but without the dermal coverage of the costal. **Bottom left)** *Physignathus lesueurii* rib (YPM HERR.016670). A1, A2) Gross morphology of rib in A1) dorsal and A2) lateral view. Black arrows mark the planes of histological sectioning, but only histological images of one distal section (B1, B2) are shown. B1) Transverse section in normal transmitted and B2) cross-polarized light. Sharpey's fibers (ShF) pertaining to the intercostal musculature are present in both the anterior and posterior parts but not in the ventral part of the rib. **Bottom right)** Bone histology of *Cyclopes didactylus* rib (YPM MAM.007543). A1,A2) Gross anatomy of the rib in A1) dorsal, and A2) lateral view. Black arrows in A2 mark the planes of sectioning. B1-B3) Proximodistal series of planes of sectioning in normal transmitted light. Note successive flattening of the rib. C1, C2) Close-ups of the anterior and posterior parts of the rib (as indicated by rectangles in B3) in cross-polarized light. Sharpey's fibers (ShF) pertaining to the reduced intercostal musculature are visible both in the anterior and posterior flanks of the ventral-most part of the rib.

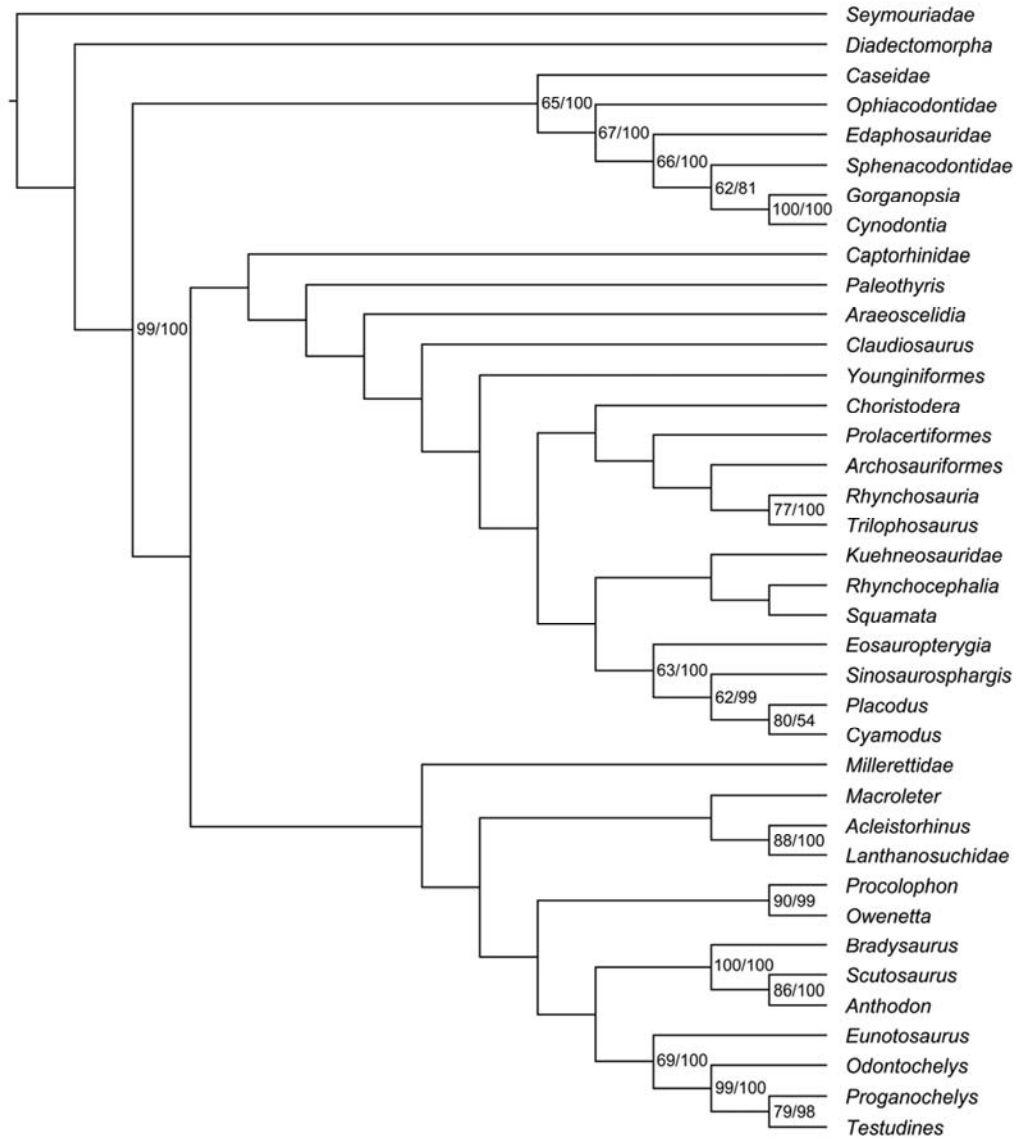


Figure S3. Results of the phylogenetic analyses, Related to Figure 4

Two most parsimonious trees (CI=0.3333, RI=0.6785, RC=0.2262) with 723 steps were obtained. Numbers above each node represent bootstrap support values whereas numbers below each node represent posterior probabilities from the Bayesian analysis.

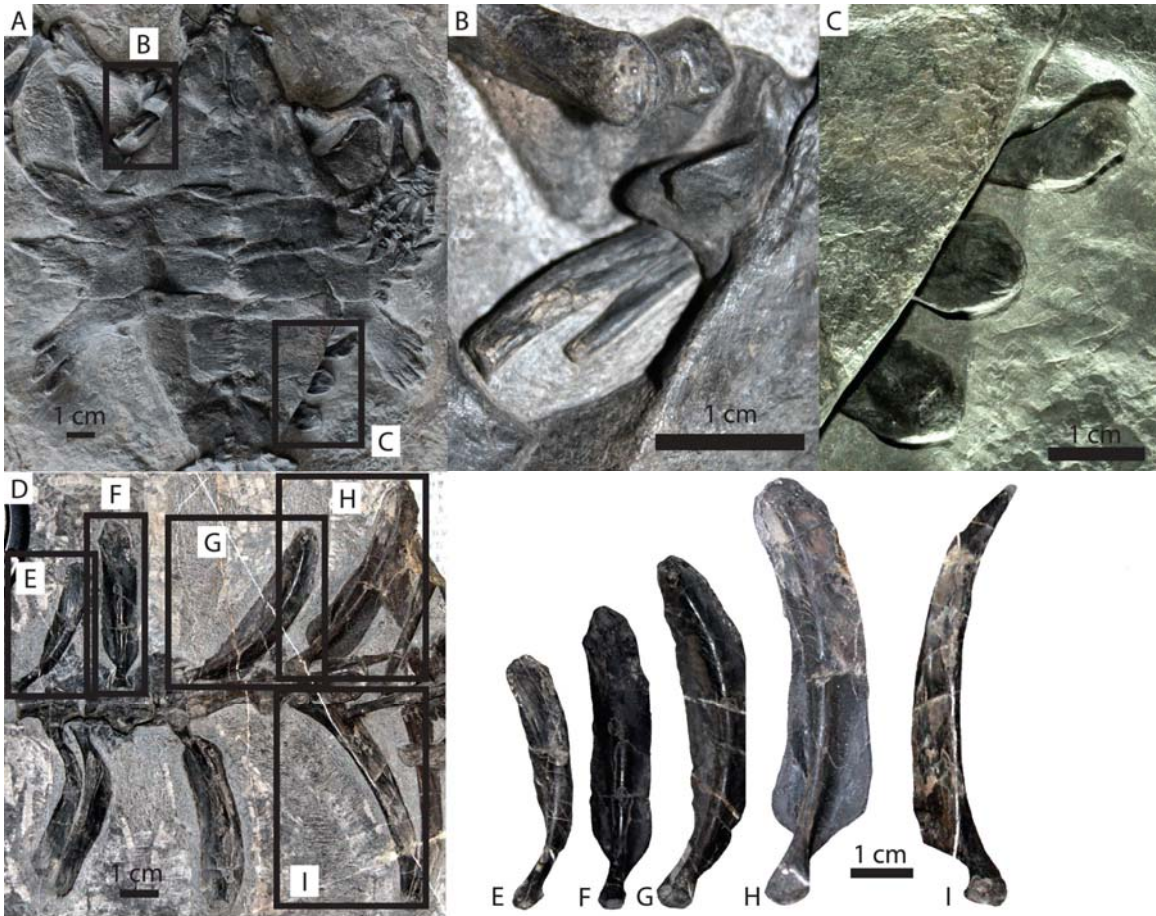


Figure S4. Photographs of *Odontochelys semitestacea*, Related to Figure 4

A) Ventral view of IVPP V 13240 with close-ups of anterior (B) and posterior (C) ribs. B) Close-up of the posterolaterally oriented anterior dorsal ribs. C) Close-up of the posterior dorsal ribs, which are oriented slightly posterolaterally. D) A disarticulated dorsal ribcage of *O. semitestacea* (IVPP V 15653). E-H) Close-ups of the left sixth (H), seventh (G), eighth (F) and ninth (E) dorsal ribs in ventral view. I) Right sixth rib in lateral view.

Supplemental Experimental Procedures

I. Materials and Methods – List of Fossil Material Examined by the Authors

Thirty-seven specimens of *Eunotosaurus africanus* collected from the *Tapinocephalus* and *Pristerognathus* Assemblage Zones (latest Guadalupian; ~260 mya) of the Karoo Basin, South Africa (see [S1]) were examined. Additional mechanical preparation was performed on GM 86/341 and GM 777. Several specimens (GM 86/341, GM 777, and QR 3299) were CT scanned and their anatomy examined digitally. The goal here is not an exhaustive description of *Eunotosaurus* but rather one focused on shell-related features and novel morphologies not apparent in previous descriptions (Fig. 1; e.g., [23, 30]). A more comprehensive treatment will be provided in a later publication.

Institutional Abbreviations: AM = Albany Museum, Grahamstown, South Africa; BPI = Bernard Price Institute, Johannesburg, South Africa; (B)NHM = Natural History Museum, London, UK; GM = Council for Geosciences, Pretoria, South Africa, GPIT = Paläontologische Lehr- und Schausammlung, University of Tübingen, Germany; IVPP = Institute for Vertebrate Paleontology and Paleoanthropology, Beijing, China; MCZ = Museum of Comparative Zoology, Harvard University, Cambridge, Massachusetts, USA; MNA = Museum of Northern Arizona, Flagstaff, USA; NMQR = National Museum, Bloemfontein, South Africa; SAM = South African Museum, Cape Town, South Africa; TMM = Texas Memorial Museum, Austin, Texas, USA; UCMP = University of California Museum of Paleontology, Berkeley, California, USA; USNM = United States National Museum, Washington DC, USA; SMNS = Staatliches Museum für Naturkunde Stuttgart, Stuttgart, Germany.

Eunotosaurus africanus:

- AM 5999: impression of a nearly complete articulated specimen with an articulated shoulder girdle, including cleithra.
- BPI 1/7198: disarticulated ribs and vertebrae.
- BPI 1/7027: fragmentary ribs and vertebrae.
- BPI 1/7024: posterior two thirds of an axial skeleton.
- BPI 1/6218: posterior two thirds of an axial skeleton and portions of the pelvis.
- BPI 1/5677: fragmentary ribs and vertebrae.
- BPI 1/3514: disarticulated dorsal vertebrae and ribs.
- BPI 1/3515: disarticulated dorsal vertebrae and ribs.
- (B)NHM R 1968 (Holotype): disarticulated dorsal vertebrae and associated dorsal ribs and associated limb elements.
- (B)NHM R 4949: disarticulated dorsal vertebrae and associated dorsal ribs.
- (B)NHM R 4054: nodule containing articulated dorsal vertebrae and ribs.
- (B)NHM R 49424: nodule containing articulated dorsal vertebrae and ribs.
- (B)NHM R 49423: highly eroded nodule containing partial dorsal vertebrae and ribs.
- GM 71: articulated dorsal vertebrae and ribs.
- GM 86/341: beautifully preserved partial skull, completely articulated neck with a few cervical ribs, and complete carapace (nine dorsal vertebrae and nine pairs of dorsal ribs) (Fig. 1, Fig. S1).

(G)M 775: articulated posterior dorsal vertebrae and ribs.
(G)M 777: articulated skull, neck, elongate cervical ribs, shoulder girdle (including cleithra), limb elements, and anterior half of carapace including dorsal vertebrae and ribs.
NMQR 3299: mostly complete skeleton including an articulated shoulder girdle, including cleithra (Fig. 1; Fig. S1)
NMQR 3466: isolated dorsal rib.
NMQR 3474: impression of a mostly articulated skeleton.
NMQR 3486: isolated dorsal rib.
NMQR 3490: isolated dorsal rib.
NMQR 3500: isolated dorsal rib.
Prince Albert Museum: mostly complete skeleton including an articulated shoulder girdle and pelvis.
SAM K 207: plastically deformed, articulated dorsal ribs and vertebrae.
SAM K 1132: mostly complete series of dorsal ribs and vertebrae with partial shoulder girdle.
SAM K 1133: complete shell with articulated shoulder girdle, including cleithra. (Fig. S1)
SAM K 7611: plastically deformed, articulated dorsal ribs and vertebrae.
SAM K 7670: highly weathered nodule with mostly complete skeleton including anterior two-thirds dorsal ribs and vertebrae, impressions of the cervical vertebrae, and an impression of the skull.
SAM K 7909: weathered nodule complete shell with articulated neck, impression of the skull, complete shoulder girdle, including cleithra (Fig. S1).
SAM K 7910: plastically deformed, articulated series of dorsal ribs and vertebrae.
SAM K 7911: mid-series section of articulated dorsal vertebrae and ribs.
SAM K 4328: impression of back two-thirds of an articulated specimen including dorsal ribs, vertebrae, partial pelvis, and first few caudal vertebrae.
SAM K 11954: highly weathered nodule containing mid-section with dorsal vertebrae and ribs.
SAM K 1509: mid-series section of articulated dorsal vertebrae and ribs.
SAM K 1673: isolated dorsal rib.
USNM 23099: disarticulated dorsal ribs, vertebrae, limb elements, pelvic girdle, and carpal and tarsal elements.

Kayentachelys aprix:

MCZ 8917: mostly complete skeleton, including complete epiplastron
MCZ 8986: partial skeleton with disarticulated epiplastron and entoplastron
MNA V1558 (Holotype): partial shell
MNA V1563: fragmentary skeleton including partial hypoplastron, entoplastron and right and left epiplastra.
TMM 43658-1: partial skeleton consisting of disarticulated shell and limb elements, including articulated fragment of anterior plastron lobe consisting of medial epiplastral portions and anterior half of entoplastron.
UCMP 150073: partial shell with almost complete articulated anterior plastral

lobe without dorsal processes of epiplastra preserved.
UCMP 150074: partial skeleton consisting of almost complete plastron, including entoplastron and left epiplastron lacking the dorsal process.

Milleretta rubidgei:

BPI 1/2040: Fifteen presacral vertebrae with articulated ribs, pelvis, femur, and gastralium.

BPI 1/2610: skull with articulated shoulder girdle.

BPI 1/3821: mostly complete postcranial juvenile skeleton with articulated shoulder girdle, vertebrae, ribs, and pelvis.

Odontochelys semitestacea:

IVPP V15639: holotype, complete skeleton.

IVPP V13240: paratype, complete skeleton.

IVPP V15653: referred specimen, disarticulated skeleton (Fig. S4)

Proganochelys quenstedti:

GPIT (uncataloged holotype): internal mold of shell showing dorsal epiplastral processes but lacking posterior margins of carapace and anterior and posterior margins of plastron.

SMNS 10012: partial carapace with internal surface and external surface preserved in separate pieces.

SMNS 15759: crushed skull, mandibles, and right half of shell.

SMNS 16980: nearly complete skeleton.

SMNS 17203: carapace and plastron.

SMNS 17204: carapace and plastron.

II. Materials and Methods/Results – Histology

Thin-sections were prepared from two specimens of *Eunotosaurus africanus* (GM 86/341; Fig. 2a-e, a left dorsal rib 3; NHM PV R 4949, Fig. S4, a left dorsal rib 7), a *Proganochelys quenstedti* costal (MB.R. 3449.2; Fig. 2h,i; right costal 7?), a lizard (*Physignathus lesueurii*) dorsal rib (YPM HERR.016670; Fig. S7), a silky anteater (*Cyclopes didactylus*) rib (YPM MAM.007543; Fig. S8), and a trionychid turtle (*Apalone ferox*) costal 6 (YPM HERR.010586; Fig. S6). The section GM 86/341 was taken near the proximal end of the rib, close to the midline (Fig. 2a, f), NHM PV R 4949 was sectioned at three different planes at proximal, mid, and distal levels (see Fig. S1). The *Proganochelys* section represents a more distal portion of the rib (Fig. 2g) comparable to the distal sections of the *Eunotosaurus* rib NHM PV R 4949. The petrographic thin-sections were prepared using standard procedures [S2] and analyzed using a LEICA DM 2500 M composite microscope, equipped with a LEICA DFC420 C digital camera. Processing and preparation of images was accomplished using ADOBE Photoshop and Illustrator.

Initial phase of bone deposition – A large cavity is visible in the center of the “midshaft region”—the most constricted part of the visceral aspect of the rib (Fig. 2b). In the more proximal sections of the ribs, this cavity is ovoid due to initial remodeling, with the long

axis of the cavity extending vertically (see NHM PV R 4949, Fig. S2). In the more distally situated sections of rib NHM PV R 4949, it is apparent that the central cavity is circular, representing the original size and shape of the cartilaginous rib primordium (Fig. S2). A zone of periosteal parallel-fibred bone (PFB) lines this cavity and gains a small degree of thickness ventrally. The layer of PFB directly adjacent to the cavities shows signs of remodeling in the form of erosion cavities partly lined with secondary lamellar bone.

First successive phase of bone deposition – Dorsally, thin sheets of anteriorly and posteriorly extending bone and interior trabeculae spread out from the bone around the central ovoid cavity. These protrusions of bone form the visceral and external part of the broadened, horizontal blade of the rib, creating a diploe structure. The external and internal/visceral sheets of bone (the latter being locally affected by remodeling) are composed of parallel-fibred bone tissue grading into lamellar bone tissue (PFB-LB). This tissue is vascularized by proximodistally or obliquely arranged, scattered, simple primary vascular canals. The interior trabeculae remain mostly composed of primary PFB but do show various stages of remodeling into secondary lamellar bone tissue. In the interior trabeculae, bone-cell lacunae are rounded to ovoid, whereas in the secondary lamellar tissue, they are more elongated and oblong in shape. A few inconspicuous Sharpey's fibers are present locally in GM 86/341, but only in the posterior shaft region.

Second successive phase of bone deposition – In the ventral aspect of the rib, the primary “ring” of bone around the central ovoid cavity is bordered by a second successive phase of bone deposition. This deposition is most pronounced ventrally, forming a drop-shaped bulge of the ventral shaft. The cortical bone deposited in this phase is composed of PFB. The tissue is vascularized by scattered simple primary vascular canals. At the terminal bulge, the vascular canals extend obliquely toward the outer bone surface. The interior bone of the bulge, on the other hand, consists of highly vascularized woven bone. Bone-cell lacunae are large and round here.

Bone deposition tapers off towards the dorsal diploe part of the rib posteriorly, about mid-height of the central ovoid cavity. Anteriorly, however, the bone tissue continues along the primary “mid-shaft region” and extends further toward the primary ventral sheet of bone of the diploe in the form of a single bone extension, which was damaged during fossilization. In the posterior part of the broadened aspect of the rib, the secondary bone layer forms a thin trabecular ovoid structure, whose ventral part has broken off and was slightly dislocated during fossilization. Inconspicuous Sharpey's fibers are again present locally only at the posterior margin of the drop-shaped bulge of the ventral shaft.

III. Materials and Methods – Phylogenetic Analysis

The debate surrounding the position of turtles has focused on three primary hypotheses. Nuclear and mitochondrial data (e.g., [12-14]) typically infer turtles as sister to Archosauria (= Aves + Crocodylia), a position that has minimal morphological support (e.g., [S3]). More comprehensive morphological studies regularly place turtles either with lepidosaurs (= Squamata plus *Sphenodon*; e.g., [25, 34, S4-5]) or outside of Diapsida (= Archosauria + Lepidosauria; e.g., [11, S6-7]). The turtle + lepidosaur clade is also

supported by microRNA data [15], whereas the turtle + diapsid clade garners additional support from some developmental data [S8].

We performed a maximum parsimony analysis on the dataset (Supplemental Experimental Procedures, sections IV, V, and VI) using PAUP 4.0b10 [S9] with all characters unordered and unweighted, as in the original analysis by deBraga and Rieppel [34]. ‘Seymouridae’ and ‘Diadectomorpha’ were specified as the outgroup taxa and a heuristic search was conducted using tree-bisection-reconnection (TBR) branch swapping with 1000 replicates of random stepwise sequence addition. Minimum branch lengths were set to collapse. Support for each node was measured by calculating bootstrap frequencies [S10], with 1000 bootstrap replicates and 1000 random sequence addition replicates.

In addition, we performed a Bayesian analysis on the dataset using MrBayes (v. 3.2.1; [S11-12]) under the Markov k (Mk) model of morphological evolution [S13] with variable character coding and a gamma rate variation distribution. Seymouridae was specified as the single outgroup. The analysis was run for 10 million generations with two simultaneous runs and four Metropolis coupling chains (three heated, one cold; $T = 0.1$), sampled every 1000 generations. Convergence was determined using the standard MrBayes diagnostics (average standard deviation of split frequencies < 0.01 , no trend in generation vs. log probability plot, Potential Scale Reduction Factor (PSRF) = 1.000 for all parameters) and in Tracer (v. 1.5; [S14]), which displayed relatively constant mean and variance in the generation vs. parameter trace plots, indicating well mixed Markov chains that had reached stationarity. A standard 25% burn-in was used in all cases.

IV. Materials and Methods – Description of Morphological Characters used in the Phylogenetic Analysis

1. Number of dorsal ribs: more than ten (0): ten or fewer (1).
2. Distinctly broadened ribs: absent (0); present, ten or more dorsal ribs broadened (1); present, nine or fewer dorsal ribs broadened (2).

Comment: We refer to costals as dorsal ribs that have broadened and sutured together as a result of metaplastic ossification. Thus all unequivocal Pantestudines have costals with the exception of *Odontochelys semitestacea* and the leatherback turtle, *Dermochelys coriacea*.

Distinctly broadened dorsal ribs are found in several amniote groups including the marine placodonts, *Eunotosaurus africanus*, and all turtles (i.e. costals). Within undisputed turtles the number changes from nine found in *Odontochelys semitestacea* and *Proganochelys quenstedti* (same as in *E. africanus*), to eight found in crown turtles [S15].

3. Outgrowth of dermal bone from the perichondral collar of the dorsal rib: absent, dorsal ribs have endochondral ossification (0); present, dermal bone grows out of the perichondral collar of the dorsal rib (1).

Comment: we scored taxa with ribs that are oval or round in cross section as having the basal condition as there is no evidence for the derived condition. We scored *Sinosaurosphargis yunguiensis* [S16] as “?” as we were unable to obtain histological data to determine if the unique cross sectional T-shape observed owed its existence to dermal bone growing out of the perichondral collar of the ribs or was the result of its pachyostotic nature.

4. Dorsal rib shape in lateral view: dorsal ribs distinctly curved (0); dorsal ribs nearly straight (1).
 Comment: this character is meant to encapsulate the axial arrest of the ribs during development.
5. Shape of distal end of dorsal ribs: blunt, indicating presence of ventral ribs or sternum (0); smooth and tapered, indicating loss of ventral ribs or sternum (1).
6. Flabellate, or fan shape, arrangement of dorsal ribs: absent, dorsal ribs are roughly parallel to each other for their entire length (0); present, distal ends of dorsal ribs are further away from each other than proximal ends (1). Comment: the derived condition is exaggerated in trionychid (soft-shelled) turtles.
7. Sharpey's fibers present on ventral portion of dorsal ribs: absent, Sharpey's fibers present on lateral edges of ribs, but Sharpey's fibers do not extend onto the ventral portion of rib (0); present, Sharpey's fibers present on ventral portion of ribs, often asymmetrically (1).
8. Neural spines of dorsal vertebrae distinctly broadened to form neurals: absent (0); present (1).
9. Clavicle and interclavicle incorporated into an immobile, bony plastron: absent (0); present (1).
10. Gastralial: segmented (0); lateral and/or medial element(s) (1); paired gastralial lacking lateral and medial portions (2)
11. Incorporated of gastralial into a bony plastron: absent (0); present (1).
12. Dorsal osteoderms overlying ribcage: not sutured together (0); sutured together (1).
13. Peripheral bones (dermal ossification lateral to the ribcage offset from a scale): absent (0); present (1).
 Comment: peripheral bones appear to be derived osteoderms found only in basal (crownward of Odontochelys) and crown turtles.
14. Number of ventral dermal ossifications exclusive of shoulder girdle: over ten (0); ten or fewer (1).
15. Osteoderms ventral to gastralial: absent (0); present (1).

V. Materials and Methods – Phylogenetic Analysis Character/Taxon Matrix for Additional Characters

Seymouriadae:	000000?000	0?000
Diadectomorpha:	000000?00?	??0?0
Caseidae:	000000?00?	??0?0
Ophiacodontidae:	000000?00?	??0?0
Edaphosauridae:	000000?00?	??0?0
Sphenacodontidae:	000000?00?	??0?0
Gorganopsia:	000000?00?	??0?0
Cynodontia:	0(01)?000?00?	??0?0
Captorhinidae:	000000?00?	??000
<i>Paleothyris</i> :	000000?00?	??000
Millerettidae:	01?000?002	0?000
<i>Acleistorhinus</i> :	??????????	?????
Lanthanosuchidae:	??????????	?????

<i>Macroleter:</i>	????????? ??0?
<i>Bradysaurus:</i>	00000?00? ?00??
<i>Scutosaurus:</i>	00000?00? ?00??
<i>Anthodon:</i>	00000?00? ?10??
<i>Procolophon:</i>	00000?002 0?000
<i>Owenetta:</i>	00000?00? ??0?0
<i>Araeoscelidia:</i>	00000?00? ??0?0
<i>Claudiosaurus:</i>	00000?00? ??0?0
Younginiformes:	00000?00? ??0?0
Kuehneosauridae:	00000?00? ??0?0
Rhynchocephalia:	00000?001 0?000
Squamata:	000000000? ??0?0
Choristodera:	00000?001 0?000
Rhynchosauria:	00000?001 0?000
Prolacertiformes:	00000?00? ??0?0
<i>Trilophosaurus:</i>	00000?00? ??0?0
Archosauriformes:	00000?001 00000
<i>Sinosaurosphargis:</i>	01??00?001 01001
<i>Placodus:</i>	00000?001 01001
<i>Cyamodus:</i>	00000?001 01001
Eosauropterygia:	00000?001 0?000
<i>Eunotosaurus:</i>	1210001002 0?010
<i>Odontochelys:</i>	12?110?112 1?010
<i>Proganochelys:</i>	1211111112 1?110
Testudines:	1211111112 1?110

VI. Materials and Methods – Phylogenetic Analysis Scoring for Additional Taxon

Sinosaurosphargis: 1000?00000 10?00????? ?0100100?2 00001????? 1?????0020
02212????? 0?1??????? ?10??112?1 020?????1?? ?010100?10 0?01?1111?
????1?00010 1????????11 ?0????????? ?????????? ?????????? ?000201001 1001?201??
00?0010100 1

VII. Materials and Methods – Kuratani et al.’s [9] Model for the Origin of the Turtle Shell

Kuratani et al. [9] proposed a model for the origin of the turtle shell that integrates the morphology of established basal turtles (particularly *Odontochelys semitestacea*) with gross and molecular developmental data. The model predicts the timing of specific developmental and morphological transformations in the lineage leading directly to the turtle crown. This includes transformations phylogenetically deep to *O. semitestacea*. The model is based largely on the timing of development data, with the fossil record (when present) used to corroborate the sequence of events. There are three major components to the model:

1. The scapula in the common ancestor of *Odontochelys semitestacea*, *Chelydra serpentina*, and *Chelus fimbriatus* will be oriented vertically and positioned rostral to the ribcage [9].

2. Axial arrest of the ribs evolved concurrent with the embryonic carapacial ridge, thus allowing the plastron to arise dermally in the absence of ventral ribs and/or sternum. Kuratani et al. [9] predict that such a developmental regime was in place in *O. semitestacea*, which has short ribs that do not bend ventrally and a fully developed plastron. In addition, they reconstruct the ribs of *O. semitestacea* as approximating each other distally [2, 9]. Based on this reconstruction, *O. semitestacea* had an incomplete CR and thus lacked a fan-like arrangement of the ribs

3. Completion of the CR is correlated with a fanning out of the dorsal ribs (i.e. flabellate arrangement), which is exaggerated in trionychid turtles (including Kuratani et al.'s [9] model organism *Pelodiscus sinensis*) and partially encloses the scapula within the shell. At this stage, the body wall folds inward with the serratus anterior (AS) muscle, whose connections are established early and which now rotates under the carapace [17]. This inhibits the invasion of limb bud-derived dorsal muscles such as the latissimus dorsi (LD) and pectoralis, whose connections are established late. These muscles circumvent the carapacial ridge (CR) and establish new attachments on the nuchal and ventral portion of the clavicle, respectively [17].

VIII. Materials and Methods – Justifications of the fossil reconstructions used in Figure 4

Proganochelys quenstedti:

Reconstruction of *Proganochelys quenstedti* is based on observations of much of the fossil material as well as the detailed description and illustrations found in Gaffney [26]. *Proganochelys quenstedti* has ten dorsal ribs, nine of which are expanded into costals, and ten dorsal vertebrae. The nine posterior dorsal ribs are distinctly T-shaped in cross section (see Fig. 2, as well as the description and Fig. 75 in 26), and the underlying blue “rib” portion of the reconstruction reflects the vertical portion of the T-shaped rib. The carapacial sutures are completely obliterated due to fusion in all but one specimen (SMNS 16980). Gaffney [26] notes grooves on the visceral side of the carapace between the costal bones, which likely approximates sutures. This is confirmed in the one specimen whose sutures are visible (SMNS 16980). While peripheral bones were undoubtedly present, no sutures are visible either between costals and peripherals or between peripherals. In all turtles, the number of peripherals is correlated with the number of marginal scales. *Proganochelys quenstedti* has 16 to 17 marginal scales [26] and therefore should have had 15 to 16 peripherals. The neural series is completely fused, but we agree with Gaffney [26] that a neural series was present as the area above the vertebrae where they are located is completely ossified. We reconstructed *P. quenstedti* with nine neural bones because there are nine costal bones, but we concede that this number is fairly arbitrary as the number of neurals varies among stem and crown turtles (i.e., *Kayentachelys aprix* has 10, [S17]). Although the anterior portion of the carapace is fully fused, an independent nuchal bone was assuredly present [26].

As noted by Gaffney [26], the scapula is situated vertically, anterior to the dorsal ribs. We agree with Gaffney's [26] identification of the strong vertical pillars anterior to the scapula as dorsal processes of the clavicles, rather than cleithra (sensu [S18]).

Odontochelys semitestacea:

Our reconstruction of *Odontochelys semitestacea* is based on observations of all

described fossil material as well as the description of Li et al. [2]. *O. semitestacea* has nine dorsal vertebrae and nine pairs of dorsal ribs which are single headed and articulate on the anterior half of the vertebrae. The nine pairs of dorsal ribs are T-shaped in cross section with and the underlying “blue” portion in the reconstruction reflects the vertical portion of the T-shaped rib. Li et al [2] describe nine pairs of dorsal ribs, with all but the last pair distinctly broadened. While we agree that the last pair is not as broad as the anterior eight pairs of ribs, it still appears to be distinctly broadened (Fig. S4): much more so than the oval or rounded ribs found in most other amniotes. The orientation of the ribs in our reconstruction differs significantly from that of Nagashima et al. [17] and Kuratani et al. [9], which have the posterior ribs pointed anteriorly and the anterior ribs pointed posteriorly, resulting in all of the ribs approximating each other distally (see Fig. 6 in [9]). Based on our observation of IVPP V13240 (the paratype), the posterior ribs are oriented laterally, roughly parallel to each other. This specimen has been prepared in ventral view exposing the plastron, but on the specimen’s left side the posterior three dorsal ribs are sticking out (Fig. S4). These ribs are evenly spaced, approximately parallel to each other and are oriented laterally (Fig. S4). This is the best specimen on which to base a reconstruction, as the remaining two specimens’ ribs are completely jumbled together or completely disarticulated, making a justified inference on the orientation of the ribs impossible. Nine neurals are present on IVPP V15639. No osteoderms or peripherals are present. A fully ossified plastron made up of five pairs of dermal bones, clavicles, and interclavicle is present. We agree with Rieppel [S19], that it is not possible to determine the presence or absence of the nuchal.

As noted by Li et al. [2], the scapula is oriented vertically anterior to the dorsal ribs. Like *Proganochelys quenstedti*, large pillar-like structures interpreted as the dorsal processes of the clavicles are situated anterior to the scapula on either side of the cervical vertebrae.

Eunotosaurus africanus

Our reconstruction is based on observations of all described material, as well as several undescribed specimens (N=37). Much of the reconstruction is based on a previously undescribed specimen, GM 86/341, which includes a beautifully preserved skull, neck, dorsal ribs and vertebrae, and sacral vertebrae. This complete specimen clearly shows nine pairs of dorsal ribs and vertebrae, which differs from the traditional reconstruction of 10 pairs of dorsal ribs and vertebrae [23-24, 30-31]. However, these previous reconstructions were based on incomplete material. The new specimen preserves the most complete neck and dorsal series, which allows for the first robust reconstruction of this area. There is a distinct change in vertebral length, shape of neural spine, and rib morphology between pre-sacral vertebrae 6 and 7 (Fig. 1; Fig. S1). We argue this demarcation is the transition between cervical and dorsal vertebrae. The cervical vertebrae are short, with a bulbous neural spine (as noted by [17]) and have long, single-headed cervical ribs that are round in cross section. Cervical rib 6 (dorsal rib one according to other authors) is long, mostly round in cross section except for a small portion in the middle that is distinctly broadened (Fig. 1; Fig. S1). Thus there are six, not five, cervical vertebrae and nine, not ten, dorsal vertebrae with nine pairs of distinctly expanded dorsal ribs. The dorsal ribs are distinctly T-shaped in cross section and contact each other for most of their length. The “blue” portion in the reconstruction represents the

vertical portion of the T-shaped ribs, while the gray portion represents the horizontal portion (i.e. the subdermal portion that ossifies out of the perichondral collar of the dorsal rib) of the T-shaped ribs. The first eight pairs of dorsal ribs are oriented slightly posteriorly, while the last pair is oriented slightly anteriorly. Unlike other specimens (USNM 23099, SAM 4328, BMNH 4949), the last pair of ribs is not fused with the dorsal vertebrae, but rather articulates with the vertebrae.

Several specimens preserve a complete, articulated shoulder girdle. The scapula is situated vertically, anterior to the dorsal ribcage (Fig. S1). The clavicles are slender elements with a distinct dorsal process (Fig. S1). A slender cleithrum is present and contacts the dorsal process of the clavicle ventrally (Fig. S1).

Milleretta rubidgei

Our reconstruction is based on examination of most of the material, namely BPI 1/2610, BPI 1/3821, and BPI 1/2040, all of which have some postcranial elements. Where absent, we used features found in the closely related *Milleropsis pricei* (BPI 1/4203). As noted by Gow [S20] there are 24 presacral vertebrae. The demarcation between cervicals and dorsal vertebrae is not obvious. We reconstructed *M. rubidgei* with 6 cervicals (the basal amniote condition) and 18 dorsal vertebrae, although this may not be the case. All of the dorsal ribs are distinctly anterior-posterior broadened and are L-shape in cross section [S21]. As noted by Gow [S20], the shoulder girdle is situated vertically rostral to the ribcage. A cleithrum is present [S20]. A distinct dorsal process of the clavicle is present [S20]. At least 13 pairs of gastralia are present [S21].

Supplemental References

- S1. Modesto, S. P. (2000). *Eunotosaurus africanus* and the Gondwanan ancestry of anapsid reptiles. *Palaeontol. Afr.* 36, 15-20.
- S2. Chinsamy, A., and Raath, M. A. (1992). Preparation of bone for histological study. *Palaeontol. Afr.* 29, 39-44.
- S3. Bhullar, B. A. S., and Bever, G. S. (2009). An archosaur-like laterosphenoid in early turtles (Reptilia: Pantestudines). *Breviora* 518, 1–11.
- S4. Rieppel, O. and Reisz, R. (1999). The origin and evolution of turtles. *Annu. Rev. Ecol. Syst.* 30, 1-22.
- S5. Müller, J. (2004). The relationships among diapsid reptiles and the influence of taxon selection. In *Recent Advances in the Origin and Early Radiation of Vertebrates*, M. V. H. Arratia and R. Cloutier, eds (Verlag Dr. Friedrich Pfeil, München, Germany), pp. 379-408.
- S6. Gauthier, J., Kluge, A. G., and Rowe, T. (1988). Amniote phylogeny and the importance of fossils. *Cladistics* 4, 105-209.
- S7. Laurin, M. and Reisz, R. R. (1995). A reevaluation of early amniote phylogeny. *Biol. J. of Linnean Soc.* 113, 165-223.
- S8. Werneburg, I. and Sánchez-Villagra, M. R. (2009). Timing of organogenesis support basal position of turtles in the amniote tree of life. *BMC Evol. Biol.* 82: doi 10.1186/1471-2148-9-82.
- S9. Swofford, D. L. (2003). PAUP*. Phylogenetic Analysis Using Parsimony (*and

- Other Methods). Version 4. Sinauer Associates, Sunderland, Massachusetts.
- S10. Felsenstein, J. (1985). Confidence limits on phylogenies: an approach using the bootstrap. *Evolution* 39, 783-791.
- S11. Huelsenbeck, J. P., Ronquist, F., Nielsen, R., and Bollback, J. P. (2001). Bayesian inference of phylogeny and its impact on evolutionary biology. *Science* 294, 2310-2314.
- S12. Ronquist, F. and Huelsenbeck, J. P. (2003). MRBAYES 3: Bayesian phylogenetic inference under mixed models. *Bioinformatics* 19, 1572-1574.
- S13. Lewis, P. O. (2001). A likelihood approach to estimating phylogeny from discrete morphological character data. *Syst. Biol.* 50, 913-925.
- S14. Rambaut, A. and Drummond, A. J. (2007). Tracer v1.4. Available from <http://beast.bio.ed.ac.uk/Tracer>
- S15. Joyce, W. G. (2007). Phylogenetic relationships of Mesozoic turtles. *Bulletin of the Peabody Museum of Natural History* 48, 3-102.
- S16. Li, C., Rieppel, O., Wu, X.-C., Zhao, L.-J., and Wang, L.-T. (2011). A new Triassic marine reptile from southwestern China. *J. Vert. Paleontol.* 31, 303-312.
- S17. Gaffney, E. S., Hutchison, J. H., Jenkins, Jr. F. A., and Meeker, L. J. (1987). Modern turtle origins: The oldest known cryptodire. *Science* 237, 289-29
- S18. Joyce, W. G., Jenkins, Jr. F. A., and Rowe, T. (2006). The presence of cleithra in the basal turtle *Kayentachelys aprix*. *Fossil Turtle Research* 1, 93-103.
- S19. Rieppel, O. (2013). The Evolution of the Turtle Shell. In D. B. Brinkman, P. A. Holroyd, and J. D. Gardner eds. *Morphology and Evolution of Turtles*. (Springer, Dordrecht, The Netherlands), pp. 51-61.
- S20. Gow, C. E. (1972). The osteology and relationships of the Millerettidae (Reptilia, Cotylosauria). *J. Zool. Lond.* 167, 219-264.
- S21. Gow, C. E. (1997). A note on the postcranial skeleton of *Milleretta* (Amniota: Parareptilia). *Palaeontol. Afr.* 34, 55-57.

Palaeontology: Turtles in Transition

One of the major remaining gaps in the vertebrate fossil record concerns the origin of turtles. The enigmatic little reptile *Eunotosaurus* could represent an important transitional form, as it has a rudimentary shell that resembles the turtle carapace.

Michael S.Y. Lee

Turtles (tortoises, terrapins and sea turtles) have a very bizarre and highly modified anatomy that has long hindered attempts to decipher their evolutionary origins and relationships. The most notable feature of their highly aberrant body plan is the external shell, which incorporates vertebrae, ribs, shoulder and sometimes the pelvis. This highly derived anatomy means that morphological traits are often not readily comparable between turtles and their putative relatives, leading to numerous disputed homologies. Therefore, turtles have been particularly difficult to place within the reptile evolutionary tree [1,2]. Now, writing in this issue of *Current Biology*, Lyson and colleagues [3] undertake a re-evaluation of the neglected Permian (~260 million year old) fossil *Eunotosaurus*. Their analysis reveals that this small, stiff-bodied terrestrial reptile possessed an expanded ribcage that shares many detailed similarities with the turtle carapace [3]. The overall morphology of *Eunotosaurus* is also consistent with that of a turtle ancestor predicted by recent ontogenetic studies. These discoveries should shed light on the broader phylogenetic relationships of turtles, and the evolutionary origins of their highly distinctive body plan.

Evolutionary Relationships Turning Turtle

Despite their uniquely specialised bodies, turtles have rather primitive 'anapsid' skulls, characterised by a solid cheek region, an arrangement resembling that of early reptiles. In contrast, all other living reptiles have more advanced 'diapsid' skulls with two large openings (fenestrae) in the cheek region [4] (Figure 1). Based on skull morphology, the search for turtle ancestors historically focused on extinct anapsid-grade reptiles, the earliest and most primitive members

of the amniote radiation. One anapsid lineage, the 'parareptiles', includes three historical contenders for turtle relatives: the procolophonids — lizard-shaped reptiles with often spinose skulls [5]; the pareiasaurs — large, stout animals varying covered with armour plates [6]; and, *Eunotosaurus* — an odd little creature with a short rigid body encased in wide leaf-shaped ribs [7]. However, all putative anapsid relatives fell from favour when genomic data robustly placed turtles within diapsid reptiles, usually as sister-group to archosaurs (birds and crocodiles) [8–10]. This arrangement implied that turtles could not be related to any primitively anapsid reptiles: rather, their anapsid-like skulls must be secondary (atavistic) rather than representative of the primitive reptilian condition, and their nearest relatives should be sought amongst diapsid reptiles, notably sauropterygians, an extinct clade that includes marine reptiles such as plesiosaurs, placodonts and ichthyosaurs [11]. The sauropterygian hypothesis raised the possibility that turtles evolved in the ocean, boosted by the recent discovery of the most primitive known turtle, the small aquatic *Odontochelys* [12]. However, this hypothesis has some inconsistencies: for instance, while genomic data place turtles with archosaurs [8–10], sauropterygians are generally considered related to the other major living branch of diapsids, the lepidosaurs (lizards, snakes and tuataras) [11,12]: if both relationships are true, then turtles and sauropterygians cannot be close kin.

The emerging consensus that turtles were aberrant diapsid reptiles stymied further consideration of anapsid-grade relatives, including all parareptiles. *Eunotosaurus* was thus overlooked in recent debates on turtle origins. Analyses focused on relationships among *Eunotosaurus* and other anapsids explicitly excluded

turtles [13,14], while analyses focused on identifying turtle relatives within diapsids excluded poorly known anapsids (such as *Eunotosaurus*) [11,12].

This Gordian knot was recently cut when the striking similarities between *Eunotosaurus* and turtles were reiterated [15,16], and the two taxa were finally simultaneously included in rigorous phylogenetic analyses [15]. The results were intriguing (Figure 1A). When turtles were added to analyses of anapsids, they fell next to *Eunotosaurus* (and thus within parareptiles in general). When *Eunotosaurus* was added to analyses focusing on diapsids, it again fell with turtles, this pairing again nesting within parareptiles. There was a consistent morphological signal uniting turtles with *Eunotosaurus* in particular, and with parareptiles generally.

Eunotosaurus: No Longer a Pariah-Saur

The potential importance of *Eunotosaurus* as a transitional taxon has spurred a detailed reassessment of the carapace-like structure of this neglected reptile, known from a handful of good specimens from South Africa. In this issue of *Current Biology*, Lyson and colleagues [3] now document additional turtle-like features in *Eunotosaurus*, which encompass gross anatomy as well as fine structural detail. As in turtles, the trunk region of *Eunotosaurus* is wide and stiff, consisting of only 9 elongate vertebrae each with a pair of broadened leaf-shaped ribs (Figure 1a). Other reptiles typically have over twenty short vertebrae, each with narrow cylindrical ribs. The similarities also extend to the underside. Most reptiles have multiple longitudinal rows of rod-like bones along their belly (gastralia), whereas *Eunotosaurus* has only two rows, perhaps a precursor to the turtle plastron which similarly consists of two rows of fused bony plates.

Eunotosaurus also appears to have lost intercostal muscles (which normally extend between the ribs and are involved in breathing and

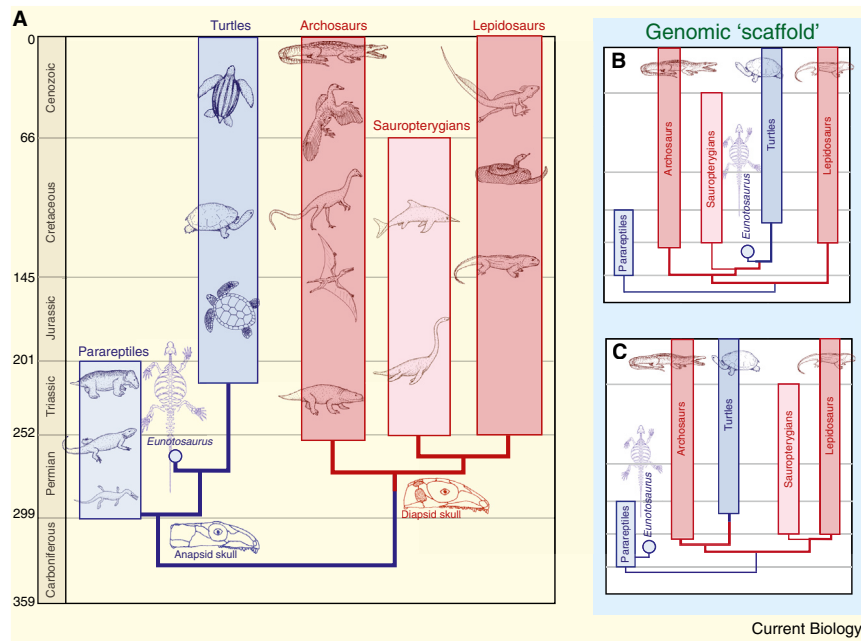


Figure 1. Phylogenetic relationships and scenarios for turtle evolution.

Affinities of *Eumotosaurs* and turtles, suggested by morphology alone (left) and morphology in the context of genomic evidence (right). Anapsid-skulled taxa in blue, diapsid-skulled taxa in red; extinct taxa in light shading, living taxa in darker shading. (A) Morphology alone suggests that *Eumotosaurs* is a stem-turtle, and places both taxa within anapsid-skulled reptiles called parareptiles, outside the clade of all diapsid reptiles (archosaurs, lepidosaurs and sauropterygians) [3,15]. However, this position conflicts with robust genomic evidence placing turtles within diapsids, next to archosaurs [8–10]. If one accepts the latter evidence, two possible resolutions to this dilemma are: (B) *Eumotosaurs* is a stem-turtle with a primitive carapace, and thus falls within the turtle-archosaur clade, perhaps along with sauropterygians; (C) alternatively, *Eumotosaurs* is an anapsid-grade parareptile, distant from the turtle-archosaur clade, and has convergently evolved numerous carapace-like traits.

locomotion), again a novel condition characteristic of turtles. The histology of the ribs of *Eumotosaurs* reveals Sharpey’s fibres (indicating muscle attachments) are only present on the ventral (i.e. internal) surface, strongly suggesting that there were no muscles extending between adjacent ribs. This inference is consistent with the short, relatively rigid ribcage of *Eumotosaurs*. Turtles, of course, have immobile ribs integrated into the carapace, and have accordingly lost intercostal musculature. Finally, microanatomy of cross-sections further suggests that the ribs of *Eumotosaurs* passed through ontogenetic stages similar to those in embryonic turtles: the ribs begin life as rod-like elements, and only later develop the leaf-shaped external expansions. The turtle-like features thus encompass both ontogeny and adult morphology.

Ontogeny Reflects Phylogeny
Based on these new analyses, the position of *Eumotosaurs* along the

ancestral turtle lineage just before *Odontochelys* (most primitive ‘true’ turtle) elucidates the order in which turtles evolved their novel adaptations [3]. Notably, the short trunk region, expanded ribs (i.e. costal bones in the turtle carapace), and reorganisation of intercostal musculature evolved very early, in the common ancestor of *Eumotosaurs* and all turtles. The dorsal plates over the vertebrae (i.e. neural bones along the carapace midline) evolved later, in the common ancestor of all turtles. This was followed by appearance of dermal bones along the edges of the carapace (peripheral bones), and envelopment of the shell around the shoulder girdle, which appeared in turtles later than *Odontochelys*.

This proposed evolutionary sequence closely matches the order in which these traits appear during the embryology of living turtles. The lateral elements (costals) of the carapace develop first, followed by the midline elements (neurals), and finally the entire developing carapace

fans out to overhang the shoulder girdle. Furthermore, development from single rather than multiple primordia suggests that costal elements evolved via broadening of ribs alone, rather than via fusion of rib and overlying armour plating [17,18]. All this ontogenetic evidence suggests that the earliest stages in the evolution of the turtle shell should be represented by an animal with only expanded ribs (costals), no neurals, a shoulder girdle anterior to a wide trunk region, and no dermal armour — precisely the *Gestalt* exhibited by *Eumotosaurs* [3].

While the new studies consistently unite *Eumotosaurs* with turtles, many questions remain. First, the striking similarities between *Eumotosaurs* and turtles are currently all associated with a single adaptive complex (the shell), raising the possibility of convergent evolution. Further study of this reptile is required, to identify turtle-like features (synapomorphies) in other anatomical areas, especially in the poorly-known skull region [16]. Such traits would more robustly corroborate the link between *Eumotosaurs* and turtles. Second, the position of the *Eumotosaurs* turtle clade within parareptiles is acknowledged to be unstable, alternating between near the lizard-shaped millerettids [15] and the large stout pareiasaurs [3]. These positions have implications for wider homologies of some major turtle novelties, e.g. some millerettids have broadened ribs and possible precursors of the turtle plastron [3,14,15], while pareiasaurs have reduced vertebral numbers and possess an ‘acromion process’, which in turtles connects the shoulder girdle with the shell [6].

However, any proposed position for *Eumotosaurs* and turtles within anapsid-grade parareptiles (Figure 1A) conflicts with the robust genomic evidence that turtles are related to archosaurs and thus nested within diapsid reptiles [8–10]. If one accepts that the molecular evidence is correct, and turtles are modified diapsids, there are two likely possibilities: *Eumotosaurs* could indeed represent the beginnings of the turtle carapace: if so, it too must fall within diapsids, and any anapsid-like features (notably in the skull) would be evolutionary reversals (Figure 1B); alternatively, *Eumotosaurs* might be a

genuinely anapsid-grade reptile which has convergently evolved several carapace-like traits (Figure 1C). These scenarios could be investigated by applying a genomic scaffold to the phylogenetic analyses: enforcing relationships among living taxa to conform to the molecular evidence (e.g. turtles as sister-group to archosaurs), and then using morphological data to best place all fossil taxa within this framework.

Whether or not the affinities of *Eunotosaurus* with turtles are eventually confirmed, the novel similarities identified in recent studies [3,15,16] will ensure that this enigmatic taxon occupies a pivotal position in future investigations. The resurrection of *Eunotosaurus* from obscurity highlights how preconceived relationships can hinder phylogenetic analyses (taxa cannot be inferred to be related if they are never simultaneously considered), and how development, genomics and the fossil record are mutually relevant.

References

1. Harris, S.R., Pisani, D., Gower, D.J., and Wilkinson, M. (2007). Investigating stagnation in morphological phylogenetics using consensus data. *Syst. Biol.* 56, 125–129.

2. Lee, M.S.Y. (2001). Reptile relationships turn turtle. *Nature* 389, 245.
3. Lyson, T.R., Bever, G.S., Scheyer, T.M., Hsiang, A.Y., and Gauthier, J.A. (2013). Evolutionary origin of the turtle shell. *Curr. Biol.* 23, 1113–1119.
4. Gauthier, J.A., Kluge, A.G., and Rowe, T. (1988). Amniote phylogeny and the importance of fossils. *Cladistics* 4, 105–209.
5. Laurin, M., and Reisz, R.R. (1995). A reevaluation of early amniote phylogeny. *Zool. J. Linn. Soc.* 113, 165–223.
6. Lee, M.S.Y. (2001). Molecules, morphology and the monophyly of diapsid reptiles. *Contrib. Zool.* 70, 1–22.
7. Watson, D.M.S. (1914). *Eunotosaurus africanus* (Seeley) and the ancestors of the Chelonina. *Proc. Zool. Soc. London* 11, 1011–1020.
8. Chiari, Y., Cahais, V., Galtier, N., and Delsuc, F. (2012). Phylogenomic analyses support the position of turtles as the sister group of birds and crocodiles (Archosauria). *BMC Biol.* 10, e65.
9. Crawford, N.G., Faircloth, B.C., McCormack, J.E., Brumfield, R.T., Winker, K., and Glenn, T.C. (2012). More than 1000 ultraconserved elements provide evidence that turtles are the sister group of archosaurs. *Biol. Lett.* 8, 783–786.
10. Wang, Z., Pascual-Anaya, J., Zadissa, A., Li, W., Nimura, Y., Huang, Z., Li, C., White, S., Xiong, Z., Fang, D., et al. (2013). The draft genomes of soft-shell turtle and green sea turtle yield insights into the development and evolution of the turtle-specific body plan. *Nat. Genet.* 45, 701–706.
11. Rieppel, O., and Reisz, R. (1999). The origin and evolution of turtles. *Annu. Rev. Ecol. Syst.* 30, 1–22.
12. Li, C., Wu, X.-C., Rieppel, O., Wang, L.-T., and Zhao, L.-J. (2008). Ancestral turtle from the late Triassic of southwestern China. *Nature* 456, 497–501.
13. Tsuji, L.A., Müller, J., and Reisz, R.R. (2012). Anatomy of *Emeroleter levis* and the phylogeny of the nycteroleter parareptiles. *J. Vert. Paleont.* 32, 45–67.
14. Cisneros, J.C., Rubidge, B.S., Mason, R., and Dube, C. (2009). Analysis of millerettid parareptile relationships in the light of new material of *Broomia perplexa* Watson, 1914, from the Permian of South Africa. *J. Syst. Palaeontol.* 6, 453–462.
15. Lyson, T.R., Bever, G.S., Bhullar, B.A.S., Joyce, W.G., and Gauthier, J.A. (2010). Transitional fossils and the origin of turtles. *Biol. Lett.* 6, 830–833.
16. Carroll, R.L. (2013). Problems of the ancestry of turtles. In *Morphology and Evolution of Turtles*, D.B. Brinkman, P.A. Holroyd, and J.D. Gardner, eds. (Dordrecht: Springer), pp. 19–36.
17. Kuratani, S., Kuraku, S., and Nagashima, H. (2011). Evolutionary developmental perspective for the origin of turtles: the folding theory for the shell based on the developmental nature of the carapacial ridge. *Evol. Dev.* 13, 1–14.
18. Hiroshi Nagashima, N., Kuraku, S., Uchida, K., Kawashima-Ohya, Y., Narita, Y., and Kuratani, S. (2012). Body plan of turtles: an anatomical, developmental and evolutionary perspective. *Anat. Sci. Int.* 87, 1–13.

Earth Sciences Section, South Australian Museum, North Tce, Adelaide 5000, Australia and School of Earth, Environmental and Landscape Sciences, University of Adelaide 5005, Australia
E-mail: mike.lee@samuseum.sa.gov.au

<http://dx.doi.org/10.1016/j.cub.2013.05.011>

Scaffolding Proteins: Not Such Innocent Bystanders

Sequential transfer of information from one enzyme to the next within the confines of a protein kinase scaffold enhances signal transduction. Though frequently considered to be inert organizational elements, two recent reports implicate kinase-scaffolding proteins as active participants in signal relay.

F. Donelson Smith and John D. Scott

Signaling networks are exquisitely organized to respond efficiently to external stimuli. Scaffolding and anchoring proteins provide a molecular framework for the integration, processing and dissemination of intracellular signals. Not surprisingly, the concept of enzyme scaffolding has profoundly influenced our thinking about how particular signaling events occur within precise intracellular environments and are insulated from promiscuous crosstalk. Early work identified scaffolds that consolidate kinase-signaling cascades. For

example, Ste5 in yeast, and the mammalian proteins KSR (kinase suppressor of Ras) and JIP (JNK-interacting protein) organize multi-enzyme MAP kinase assemblies that relay phosphorylation-dependent signals to potentiate activation of the terminal ‘transduction’ enzyme [1,2]. A variation on this theme is the family of A-kinase anchoring proteins (AKAPs) that compartmentalize combinations of signaling enzymes that respond to distinct inputs. AKAPs nucleate multimeric protein complexes that cluster signal activation components, such as G-protein-coupled receptors and protein kinases, with signal termination

enzymes, including protein phosphatases and cyclic nucleotide phosphodiesterases [3]. This permits local and reversible control of signal-dependent responses. In addition, sophisticated mathematical modeling has derived algorithms to simulate how scaffolding and anchoring proteins shape signaling events [4,5]. A common denominator has been the notion that scaffolding and anchoring proteins are passive participants that simply hold their enzyme binding partners in place. Two papers recently published in *Science* challenge this concept by demonstrating that certain ‘scaffolding’ proteins are actually active elements in the enzyme complexes that they organize [6,7].

In the first of these papers, Rock et al. [6] present exciting work on the yeast mitotic exit network (MEN) scaffold protein Nud1. This protein is an important hub in the signaling network that controls exit from mitosis during the cell cycle. Components of the